Atmos. Chem. Phys., 17, 13491–13508, 2017
https://doi.org/10.5194/acp-17-13491-2017
© Author(s) 2017. This work is distributed under
the Creative Commons Attribution 3.0 License.

Atmospheric Chemistry and Physics
Open Access
EGU

Secondary organic aerosol from chlorine-initiated oxidation of isoprene

Dongyu S. Wang and Lea Hildebrandt Ruiz

McKetta Department of Chemical Engineering, The University of Texas at Austin, Austin, Texas, USA

Correspondence to: Lea Hildebrandt Ruiz (lhr@che.utexas.edu)

Received: 14 April 2017 – Discussion started: 9 May 2017
Revised: 14 September 2017 – Accepted: 25 September 2017 – Published: 14 November 2017

Abstract. Recent studies have found concentrations of reactive chlorine species to be higher than expected, suggesting that atmospheric chlorine chemistry is more extensive than previously thought. Chlorine radicals can interact with hydroperoxy (HO_x) radicals and nitrogen oxides (NO_x) to alter the oxidative capacity of the atmosphere. They are known to rapidly oxidize a wide range of volatile organic compounds (VOCs) found in the atmosphere, yet little is known about secondary organic aerosol (SOA) formation from chlorine-initiated photooxidation and its atmospheric implications. Environmental chamber experiments were carried out under low-NO_x conditions with isoprene and chlorine as primary VOC and oxidant sources. Upon complete isoprene consumption, observed SOA yields ranged from 7 to 36 %, decreasing with extended photooxidation and SOA aging. Formation of particulate organochloride was observed. A high-resolution time-of-flight chemical ionization mass spectrometer was used to determine the molecular composition of gas-phase species using iodide–water and hydronium–water cluster ionization. Multi-generational chemistry was observed, including ions consistent with hydroperoxides, chloroalkyl hydroperoxides, isoprene-derived epoxydiol (IEPOX), and hypochlorous acid (HOCl), evident of secondary OH production and resulting chemistry from Cl-initiated reactions. This is the first reported study of SOA formation from chlorine-initiated oxidation of isoprene. Results suggest that tropospheric chlorine chemistry could contribute significantly to organic aerosol loading.

1 Introduction

Studies have shown that long-term exposure to fine particulate matter (PM), also known as aerosol, is linked to increases in mortality and cardiorespiratory diseases (Dockery et al., 1993; Pope et al., 2006). Short-term exposure to aerosol could also induce stress response and cytotoxicity in cells (de Bruijne et al., 2009; Ebersviller et al., 2012; Hawley et al., 2014). Equilibrium partitioning of oxidized, semi-volatile organic compounds (Pankow, 1994), collectively referred to as secondary organic aerosol (SOA), contributes 20–90 % of the global fine aerosol budget (Jimenez et al., 2009; Kanakidou et al., 2005). The majority of SOA originates from oxidation of biogenic volatile organic compounds (BVOCs), which account for ∼ 90% of annual non-methane hydrocarbon emissions (Goldstein and Galbally, 2007; Guenther et al., 2012), among which isoprene has the highest emission rate at $\sim 600\,\mathrm{Tg\,yr^{-1}}$ (Guenther et al., 2006). Isoprene SOA formation initiated by ozone (O_3), nitrate (NO_3), and hydroxyl (OH) radicals has been studied extensively and is estimated to account for 6–30 $\mathrm{Tg\,yr^{-1}}$ of the global aerosol budget (Brégonzio-Rozier et al., 2015; Claeys, 2004; Guenther et al., 2006; Kroll et al., 2006; Lin et al., 2012; Surratt et al., 2006, 2010; Zhao et al., 2015), but the importance of isoprene SOA formation within the marine boundary layer (MBL) remains highly disputed in the literature (Arnold et al., 2009; Bikkina et al., 2014; Fu et al., 2011, 2013; Gantt et al., 2010, 2015; Hu et al., 2013; Luo and Yu, 2010; O'Dowd and de Leeuw, 2007). Although the production of reactive chlorine species such as Cl_2 and HOCl has been observed within the MBL (Lawler et al., 2011), little is known about SOA from chlorine-initiated oxidation of isoprene.

Chlorine chemistry is known to have important effects on ozone layer depletion (Crutzen, 1974; Molina and Rowland, 1974). Recent laboratory studies and field measurements also suggest an important role of halogen (X) chemistry on tropospheric composition (Faxon and Allen, 2013; Finlayson-Pitts, 2010; Saiz-Lopez and von Glasow, 2012; Simpson et al., 2015). Reactive halogen species in the form of X_2, XO, HOX, XNO_2, and OXO are present in polar regions (Buys et al., 2013; Liao et al., 2014; Pöhler et al., 2010), the MBL (Lawler et al., 2011; Read et al., 2008), and coastal and inland regions (Mielke et al., 2013; Riedel et al., 2012, 2013). Outside of the MBL and polar regions, natural emissions of reactive halogen species have been observed in volcano plumes (Bobrowski et al., 2007) and over salt lakes (Kamilli et al., 2016; Stutz, 2002). Anthropogenic sources include industrial emissions (Chang and Allen, 2006; Riedel et al., 2013; Tanaka et al., 2003), oil and gas production (Edwards et al., 2014), water treatment (Chang et al., 2001), biomass burning (Lobert et al., 1999), engine exhaust (Osthoff et al., 2008; Parrish et al., 2009), and NO_x-mediated heterogenous reactions, notably the production of $ClNO_2$ via reactive uptake of N_2O_5 onto particles containing Cl^- (Thornton et al., 2010). Recent studies have found that models underpredict the abundance of reactive halogen species, suggesting incomplete understanding of their sources (Faxon and Allen, 2013; Faxon et al., 2015; Simpson et al., 2015; Thornton et al., 2010). Photolysis of reactive halogen species produces halogen radicals that can react with O_3, hydrocarbons, SOA, and other radicals in the atmosphere. Reactions with hydrocarbons and organic aerosols serve as chlorine and bromine radical sinks (Buxmann et al., 2015; Ofner et al., 2012; Platt and Hönninger, 2003), especially in high-NO_x environments where halogen recycling via HO_x and XO reaction pathways is suppressed (Edwards et al., 2013; Riedel et al., 2014; Simpson et al., 2015).

The concentration of chlorine radicals is estimated to be on the order of 10^2 to 10^5 molecules cm^{-3} (Saiz-Lopez and von Glasow, 2012; Wingenter et al., 1999, 2005), which is 1 to 3 orders of magnitude lower compared to OH radicals under ambient conditions (Faxon and Allen, 2013; Wingenter et al., 1999), but due to its high reactivity towards numerous VOCs, chlorine radicals could contribute significantly as a primary oxidant under certain conditions (Riedel et al., 2012; Riva et al., 2015; Young et al., 2014). Hydrogen abstraction and chlorine addition to VOCs produce peroxy and chloroperoxy radicals, respectively, that could lead to the production of secondary HO_x radicals and the formation of semi-volatile oxidized products. Studies have shown that chlorine-initiated oxidation of α-pinene (Cai and Griffin, 2006; Ofner et al., 2013), toluene (Cai et al., 2008; Huang et al., 2014; Karlsson et al., 2001), and polycyclic aromatic hydrocarbons (PAHs; Riva et al., 2015) leads to SOA formation, with SOA yields close to unity reported for select PAHs (Riva et al., 2015). Reactive chlorine species could also enhance OH-radical propagation (Young et al., 2014), nocturnal NO_x recycling (Riedel et al., 2012; Thornton et al., 2010), and ozone production (Tanaka et al., 2003), further increasing the oxidative capacity of the atmosphere.

Chlorine-initiated oxidation of isoprene could either proceed via the dominant (85 %) chlorine-addition pathway or a minor (15 %) hydrogen-abstraction pathway (Fantechi et al., 1998; Lei and Zhang, 2000; Nordmeyer et al., 1997; Orlando et al., 2003). Major gas-phase products include methyl vinyl ketone (MVK), methacrolein (MACR), chloroacetone, chloroacetaldehyde, hydrochloric acid, and isomers of 1-chloro-3-methyl-3-butene-2-one (CMBO), a unique tracer for atmospheric chlorine chemistry (Nordmeyer et al., 1997; Riemer et al., 2008; Tanaka et al., 2003). The rate constant of the isoprene–chlorine reaction at 25 °C (2.64–5.50×10^{-10} molecules^{-1} cm^3; Fantechi et al., 1998; Orlando et al., 2003; Ragains and Finlayson-Pitts, 1997) is much larger than the rate constant of the isoprene–OH reaction (1.00×10^{-10} molecules^{-1} cm^3; Atkinson and Arey, 2003), suggesting that isoprene–chlorine chemistry could compete with isoprene–OH chemistry under certain conditions. Moreover, reactions between chlorine and isoprene or isoprene-derived SOA could serve as a reactive chlorine sink in the atmosphere, as has been proposed for reactions between chlorine and biogenic SOA (Ofner et al., 2012). To our knowledge, SOA formation from chlorine-initiated oxidation of isoprene has not been reported in the literature. In order to address this significant knowledge gap, environmental chamber experiments were conducted using chlorine radicals as the primary oxidant source for isoprene oxidation. Experiments were conducted under low-NO_x conditions, using neutral or acidified seed aerosol to evaluate the effect of aerosol acidity on SOA formation. The mass yields and composition of SOA formed from chlorine-initiated oxidation of isoprene are reported for the first time. Formation of organochlorides was also observed. Gas-phase measurements provide evidence of multi-generational oxidation chemistry, secondary HO_x chemistry, and multifunctional gas-phase products.

2 Methods

2.1 Environmental chamber experiments

Experiments were performed at 25 °C under low relative humidity (RH < 10 %) and low-NO_x (< 5 ppb) conditions in a 12 m^3 temperature-controlled Teflon® chamber lined with UVA lights. Chamber characteristics were described elsewhere (Bean and Hildebrandt Ruiz, 2016). The UV spectrum is similar to other blacklight sources reported in the literature (Carter et al., 2005). The NO_2 photolysis rate is used to characterize UV intensity and was determined to be 0.5 min^{-1}, similar to ambient levels (e.g., 0.53 min^{-1} at 0° zenith angle; Carter et al., 2005). Temperature, RH, and the concentrations of O_3, NO, NO_2, and NO_x were continuously monitored. The chamber was flushed with dry clean air gen-

erated by a clean air generator (Aadco, 737R) at a flow rate exceeding 100 L min^{-1} for at least 12 h before each experiment. Between experiments, "blank experiments" were conducted in which seed particles, O_3, and Cl_2 (Airgas, 106 ppm in N_2) were injected into the chamber at high concentrations and UV lights were turned on to remove any residual organics which could be released from the Teflon® chamber surface. Background effects have been quantified using chamber characterization experiments (Carter et al., 2005) and the SAPRC chamber modeling software (http://www.engr.ucr.edu/~carter/SAPRC/) in combination with the Carbon Bond 6 (CB6r2) chemical mechanism, which was modified to include basic gas-phase inorganic chlorine chemistry in addition to Cl_2 and $ClNO_2$ photolysis (Sarwar et al., 2012; Yarwood et al., 2010). NO_x off-gasing is represented within the model by a constant emission of nitrous acid (HONO) from the chamber walls on the order of 0.1 ppb min^{-1}, which was determined separately in chamber characterization experiments (Carter et al., 2005).

For each experiment, microliters of isoprene (Acros Organics, 98 % stabilized) were transferred into a glass sampling tube (Kimble-Chase, 250 ml), which was then flushed with clean air into the chamber. Depositional particle wall loss was constrained using dried, monomodal, and polydisperse seed particles introduced prior to photooxidation using an aerosol generation system (Brechtel, AGS model 9200). Neutral seed particles were generated from a 0.01 M ammonium sulfate solution; acidic seed particles were generated using a solution containing 0.005 M ammonium sulfate and 0.0025 M sulfuric acid. Two Cl_2 injection methods were used: for "initial Cl_2" experiments, all Cl_2 was injected in the dark and allowed to mix with isoprene prior to photooxidation. For "continuous Cl_2" experiments, Cl_2 was injected continuously with UV lights on at 0.1 L min^{-1} with an additional 0.9 L min^{-1} clean air dilution flow, equivalent to $\sim$0.88 ppb min^{-1} Cl_2 into the chamber. Initial Cl_2 experiments were performed to achieve rapid oxidation of isoprene and to separate initial SOA formation from effects of vapor wall loss. Because chlorine radicals are not expected to regenerate, continuous Cl_2 injection experiments were performed to provide more steady but lower chlorine radical concentrations.

2.2 Instrumentation

A high-resolution time-of-flight chemical ionization mass spectrometer (CIMS; Aerodyne Research Inc.) was used to measure gas-phase organic compounds. Detailed theory and operation of the CIMS are discussed elsewhere (Aljawhary et al., 2013; Bertram et al., 2011; Lee et al., 2014; Yatavelli et al., 2012). Reagent ions are generated by passing humidified UHP N_2 over a methyl iodide permeation tube and then through a ^{210}Po radioactive cartridge (NRD, P-2021) at 2 L min^{-1} into the ion–molecule reaction (IMR) chamber operating at 200 mbar pressure. Analyte, "M" can undergo chemical ionization within the IMR with hydronium–water, $(H_2O)_n(H_3O)^+$, or iodide–water, $(H_2O)_nI^-$ ion clusters,

$$(H_2O)_n(H_3O)^+ + M \rightarrow (H_2O)_n(MH)^+ + H_2O, \quad (1)$$

$$(H_2O)_nI^- + M \rightarrow (H_2O)_n(MI)^-, \quad (2)$$

where the number of clusters, "n" ranges from 0 to 2 for $(H_2O)_n(H_3O)^+$, with $(H_2O)(H_3O)^+$ being the most dominant reagent ion in the positive ion mode. Hydronium–water cluster CIMS was used to detect isoprene and select moderately oxidized species (Aljawhary et al., 2013). For $(H_2O)_nI^-$ ionization, "n" ranges from 0 to 1, with I^- being the most dominant reagent ion. Water–iodide cluster CIMS was used to detect select highly oxidized and acidic species (Aljawhary et al., 2013; Lee et al., 2014). An aerosol chemical speciation monitor (ACSM; Aerodyne Research Inc.) was used to determine the bulk chemical composition of submicron, non-refractory aerosol species (Ng et al., 2011a). Analytes are flash-vaporized at 600 °C, ionized via electron impact ionization (EI), and then measured by a quadrupole mass spectrometer (Ng et al., 2011a). Background-corrected ("difference") mass spectra are obtained by subtracting filtered ("closed") from unfiltered ("open") measurements (Ng et al., 2011a). A standard fragmentation table is used to speciate difference mass spectra (Allan et al., 2004). Calibration is performed with 300 nm size-selected ammonium nitrate and ammonium sulfate aerosol to determine the response factor for particulate nitrate and the relative ionization efficiencies (RIE) for sulfate and ammonium; these values are needed to convert ion intensities to mass concentrations (Ng et al., 2011a). Particle volume and size distributions were measured using a scanning electrical mobility spectrometer (Brechtel, SEMS model 2002) consisting of a differential mobility analyzer and a butanol condensation particle counter. SEMS sheath and sample flow rates were set to 5 and 0.35 L min^{-1}, respectively, covering a 10–1000 nm sizing range.

2.3 Data analysis

Suspended particles are lost to the Teflon® chamber wall over time, for which numerous correction methods have been proposed (Carter et al., 2005; Hildebrandt et al., 2009; Nah et al., 2017; Ng et al., 2007; Pathak et al., 2007; Pierce et al., 2008; Verheggen and Mozurkewich, 2006). Recent studies also report loss of organic vapors to Teflon® surfaces (Kokkola et al., 2014; Krechmer et al., 2016; Loza et al., 2010; Matsunaga and Ziemann, 2010; Zhang et al., 2015). Assuming internal mixing of particles and that organic vapor can condense onto suspended and wall-deposited particles alike, we corrected for particle wall loss and the loss of organic vapors onto wall-deposited particles using the organic-to-sulfate ratio (Hildebrandt et al., 2009),

$$C_{OA}(t) = \frac{C_{OA}^{sus}(t)}{C_{seed}^{sus}(t)} C_{seed}^{sus}(t=0), \quad (3)$$

where $C_{\mathrm{OA}}^{\mathrm{sus}}(t)$ is the suspended organic aerosol (OA) concentration, which was zero at the start of each experiment, $C_{\mathrm{seed}}^{\mathrm{sus}}(t)$ is the suspended seed particle concentration, $C_{\mathrm{seed}}^{\mathrm{sus}}(t=0)$ is the suspended seed particle mass concentration at the start of photooxidation, and $C_{\mathrm{OA}}(t)$ is the corrected OA concentration. This correction does not account for loss of organic vapors to clean Teflon® surfaces.

SOA yield, Y, is calculated as follows:

$$Y = \frac{C_{\mathrm{OA}}}{\Delta \mathrm{VOC}}, \tag{4}$$

where ΔVOC is the amount of VOC consumed. Based on absorptive equilibrium partitioning theory (Odum et al., 1996; Pankow, 1994), the volatility basis set (VBS) framework (Donahue et al., 2006) states that

$$Y = \xi = \sum_i \alpha_i \xi_i, \tag{5}$$

$$C_i = \alpha_i \Delta \mathrm{VOC}, \tag{6}$$

$$\xi_i = \left(1 + \frac{C_i^*}{C_{\mathrm{OA}}}\right)^{-1}, \tag{7}$$

$$C_{\mathrm{OA}} = \sum_i C_i \xi_i, \tag{8}$$

where C_i^* is the effective saturation concentration of the surrogate compound in VBS bin i in $\mu g\,m^{-3}$; α_i, C_i, ξ_i are the total yield, total mass concentration, and the condensed-phase mass fraction of bin i, respectively. By rearranging Eqs. (5)–(8), an expression for the minimum VOC consumption required for SOA formation can be derived (see Sect. S1 in the Supplement):

$$(\Delta \mathrm{VOC}_{\mathrm{min}})^{-1} = \sum_1^n \frac{\alpha_i}{C_i^*}, \tag{9}$$

where $\Delta \mathrm{VOC}_{\mathrm{min}}$ is low if low-volatility compounds dominate the aerosol phase. When aerosol volatility is low and aerosol loading is high, such that the condensed-phase mass fraction, ξ_i, from Eq. (7) approaches 1, the "maximum" SOA yield (Griffin et al., 1999) is reached, where

$$Y_{\mathrm{max}} = \sum_1^n \alpha_i. \tag{10}$$

The extent of SOA oxidation is depicted using f_{44} and f_{43}, which represent the fractional contribution to the total organic ion signal measured by the ACSM from ion fragments at mass-to-charge (m/z) 44 (mostly CO_2^+, a proxy for doubly oxidized compounds) and at m/z 43 (mostly $C_2H_3O^+$, a proxy for singly oxidized compounds), respectively (Chan et al., 2010; Chhabra et al., 2011; Ng et al., 2011b). Based on empirical correlations, the oxygen-to-carbon ratio (O : C), the hydrogen-to-carbon ratio (H : C), and the oxidation state of carbon ($\overline{\mathrm{OS}}_{\mathrm{c}}$) can be estimated from f_{44} alone as summarized in Sect. S2 (Canagaratna et al., 2015; Donahue et al., 2012; Heald et al., 2010; Kroll et al., 2011). The empirical correlations were derived using a comprehensive collection of aerosol mass spectrometer data sets but may underestimate O : C values for SOA formed under low-NO_x conditions from isoprene or toluene (Canagaratna et al., 2015). Variability in f_{43} and f_{44} among different ACSMs has also been reported (Crenn et al., 2015).

High-resolution mass spectra fitting of CIMS data was performed using the software Tofware V2.5.7 (Tofwerk) in Igor Pro V6.37 (Wavemetrics Inc.). CIMS sensitivity correction utilized the active chemical ionization mass spectroscopy (ACIMS) formula (de Gouw and Warneke, 2007), normalizing all product ion signals against dominant reagent ion signals, $(H_2O)_nH_3O^+$ and $(H_2O)_nI^-$. For most experiments conducted, the reagent signals were at least 5 times greater than the summed product signals, equivalent to less than 10 % overcorrection by ACIMS compared to more rigorous methods such as parallel ACIMS, which accounts for reagent ion depletion (see Sect. S3 for a more detailed discussion). Because the CIMS cannot distinguish between isomers and because of the lack of calibration standards, gas-phase data presented here are normalized by the maximum signals for better visualization and evaluation of qualitative trends.

3 Results and discussion

3.1 SOA formation, aging, and composition

Table 1 summarizes the experimental conditions and results. Figure 1 compares wall-loss-corrected SOA time series from three experiments with similar precursor concentrations. In the continuous Cl_2 experiments (C2 and C7), isoprene gradually reacted away during Cl_2 injection; SOA concentration steadily increased until isoprene was depleted, at which point SOA concentration began to decay. The decay of SOA was likely due to oxidative fragmentation (Kroll et al., 2011), vapor wall loss (Boyd et al., 2015; Krechmer et al., 2016), and/or photolysis of, for example, peroxide species (Kroll et al., 2006; Surratt et al., 2006), which were observed in the gas phase (see Sect. 3.4). The initial Cl_2 experiment (A4) exhibited similar trends, but the SOA decay was faster, where 30 $\mu g\,m^{-3}$ SOA decay (40 % of maximum SOA mass) occurred within about 30 min of photooxidation (9 min $< T <$ 40 min), likely due to more rapid oxidation and fragmentation of reaction products. Under UV, the effects of oxidative fragmentation and photolysis cannot be separated from the effects of vapor wall loss. SOA decay was slower in the dark than under UV (see Sect. S2 and Fig. S1 in the Supplement). Vapor wall effects are expected to be more important when the concentrations of the oxidant and OA are lower, in which case oxidative fragmentation effects are weaker and less absorbing mass is available to compete with wall loss. After extended photooxidation ($T >$ 100 min), SOA concentrations achieved via initial Cl_2

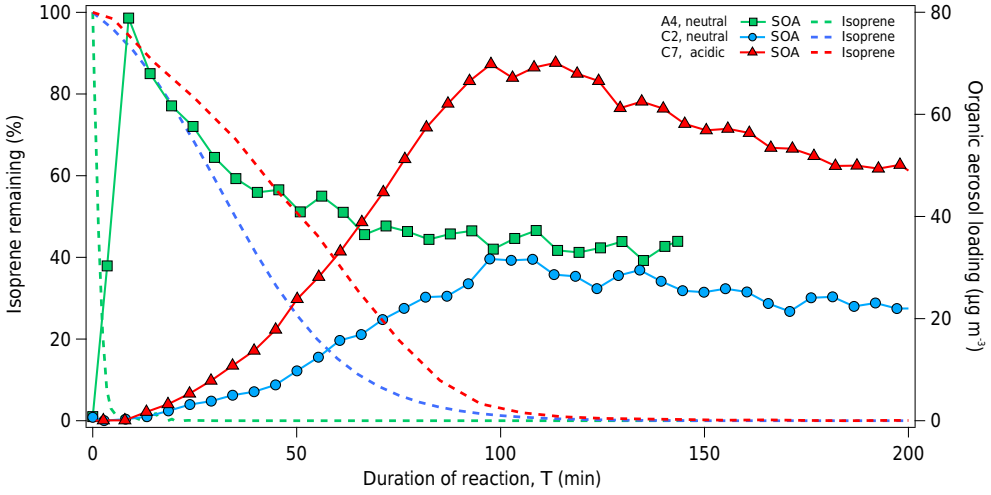

Figure 1. Comparison of SOA formation during continuous (C2, C7) and initial (A4) Cl_2 injection experiments with similar precursor concentrations but different seed aerosol acidities (C2 vs. C7). SOA concentration is wall loss corrected and averaged over 5 min intervals. Isoprene concentration is tracked using $(H_2O)_nH_3O^+$ CIMS and averaged over 1 min intervals. Maximum SOA concentrations are reached when isoprene has been depleted. After extended oxidation, observed OA loadings are similar for initial chlorine and continuous chlorine experiments using neutral seed particles. Peak SOA concentration reached in the presence of acidic aerosol during Exp. C7 is much higher than peak SOA concentration reached using neutral seed during Exp. C2.

Table 1. Summary of experimental conditions and results.

Exp.[a]	Isoprene (ppb)[b]	Chlorine (ppb)[c]	VOC : Cl_2	Cl_2 inj.[d]	Ini seed SA ($\mu m^2\ cm^{-3}$)[e]	Seed acidity	Max OA ($\mu g\ m^{-3}$)[f]	Yield
A1	24	40	0.60	Ini	1500	Neutral	12	0.18
A2	40	88	0.45	Ini	900	Neutral	23	0.21
A3	82	120	0.68	Ini	810	Neutral	39	0.17
A4	120	180	0.67	Ini	1300	Neutral	79	0.24
A5	160	230	0.70	Ini	1800	Neutral	88	0.20
A6	98	100	0.98	Ini	3700	Acidic	80	0.29
A7	98	100	0.98	Ini	2700	Acidic	70	0.26
A8[h]	180	360	0.50	Ini	780	Neutral	180	0.36
C1	40	94	0.42	Cont	950	Neutral	9	0.08
C2	120	180	0.67	Cont	880	Neutral	32	0.10
C3	240	270	0.89	Cont	770	Neutral	53	0.08
C4	300	250	1.20	Cont	1400	Neutral	60	0.07
C5[g]	73	120	0.61	Cont	NA	Neutral	NA	NA
C6	98	180	0.54	Cont	2400	Acidic	41	0.15
C7	120	150	0.80	Cont	3200	Acidic	70	0.21

[a] "A" for initial Cl_2 injection experiments and "C" for continuous Cl_2 injection experiments. [b] Initial isoprene concentration. [c] Amount of chlorine injected initially (for A1–A8) or cumulatively (for C1–C7). [d] Chlorine injection method: "Ini" for initial injection; "Cont" for continuous injection. [e] Total initial surface area of ammonium sulfate or acidified seed aerosol. [f] Highest, particle wall-loss-corrected OA concentration observed. [g] SEMS data are not available (NA) for C5. [h] ACSM scan speed for A8 (500 ms amu^{-1}) was different from other experiments (200 ms amu^{-1}).

injection (Exp. A4) and continuous Cl_2 injection (Exp. C2) differed by less than 8 $\mu g\ m^{-3}$ (< 20 % of total SOA mass at $T = 100$ min for Exp. C2). The data shown in Fig. 1 and summarized in Table 1 also suggest that aerosol acidity promotes SOA formation: the SOA concentrations observed in acidified seed Exp. C7 were more than twice as high as SOA concentrations observed in neutral seed Exp. C2. In addition, greater seed aerosol surface area appears to result in higher SOA concentrations, as shown in Table 1 for Exp. A6 and Exp. A7. The formation of SOA began shortly after UV lights were turned on in all experiments. ΔVOC_{min} from Eq. (9) is therefore small, suggesting that the initial oxidation prod-

ucts responsible for SOA formation have very low volatility. Prompt SOA formation was also observed in previous work for chlorine-initiated oxidation of α-pinene (Cai and Griffin, 2006; Ofner et al., 2013) and toluene (Cai et al., 2008; Huang et al., 2014; Karlsson et al., 2001). Formation of low-volatility early generation products may be a common feature of chlorine-initiated oxidation.

Figure 2 shows that SOA oxidation state, represented by f_{44} and estimated $\overline{\mathrm{OS}}_\mathrm{c}$, depended on the initial isoprene concentration and was unaffected by the oxidant injection method. Because isoprene is more reactive towards chlorine radicals than its oxidation products, such as MVK and MACR (Orlando et al., 2003), isoprene could scavenge radicals and delay SOA aging. Additionally, increased OA mass loading could absorb less oxidized and more volatile compounds into the particle phase, lowering the observed SOA oxidation state at higher SOA loadings resulting from higher initial isoprene concentrations. The estimated $\overline{\mathrm{OS}}_\mathrm{c}$ of chlorine–isoprene SOA increased from -0.5 to over 1 during Exp. C1, characteristic of the evolution of semi-volatile oxygenated OA (SV-OOA) to low-volatility oxygenated OA (LV-OOA; Kroll et al., 2011). Oxidation of chlorine–isoprene SOA formed under low NO_x follows a similar trajectory as OH–isoprene SOA formed in previous work under higher NO_x, which is considerably more oxidized than OH–isoprene SOA formed under low-NO_x conditions (Chhabra et al., 2011), as shown in Fig. 3. The oxidizing capacity of chlorine radicals has also been demonstrated for select biogenic SOA derived from α-pinene, catechol, and guaiacol, where halogenation led to significant SOA aging, formation of high-molecular-weight compounds, and particle growth (Ofner et al., 2012). High reactivity of chlorine radicals towards isoprene and its reaction products meant that extensive SOA processing could be easily achieved within laboratory timescales.

3.2 Particulate organochloride

Chlorine addition to the double bond is the dominant ($\sim 85\%$) isoprene–chlorine reaction pathway (Fan and Zhang, 2004; Ragains and Finlayson-Pitts, 1997), and thus the formation of semi-volatile and low-volatility chlorinated organic compounds would be expected. Aerosol analytes undergo electron impact ionization in the ACSM, and chlorine-containing ion fragments are mostly expected at m/z 35 and 37 as Cl^+ and at m/z 36 and 38 as HCl^+. Larger organochloride ion fragments may exist but cannot be separated in the unit mass resolution spectra. A previous study on chorine-initiated oxidation of toluene, which proceeds primarily through a hydrogen-abstraction pathway, reported particulate chlorine formation (4 % of the total aerosol mass), which was attributed to HCl uptake (Cai et al., 2008). Formation of organochloride aerosol has been observed previously for chlorine-initiated oxidation of α-pinene (Ofner et al., 2013), which proceeds primarily via a chlorine-addition reaction pathway. Thus, isoprene–chlorine reactions are expected to result in particulate organochloride formation. The uptake of HCl produced from hydrogen abstraction or intramolecular HCl elimination (Ragains and Finlayson-Pitts, 1997) could also contribute slightly to observed particulate chlorine. Organochloride has also been observed in biogenic SOA post-processed by halogenation (Ofner et al., 2012), in new particles formed from 1,8-cineol and limonene over simulated salt lakes (Kamilli et al., 2015), and in situ over salt lakes (Kamilli et al., 2016). To date, this is the only reported study of organochloride measurement using an ACSM.

As shown in Fig. 4 for Exp. A8, the ACSM initially observed significant levels of particulate chlorine (over 9 % of the total SOA mass), which then decreased to near-background levels. In other experiments, particulate chlorine concentrations were near the detection limit. The low observed chlorine concentration was likely due to incomplete vaporization of chlorinated compounds during the sample (open) period, resulting in particulate matter vaporization during the filter (closed) period and overestimation of background signals, as explained in more detail in section S4. Further analysis shows that while the difference signal of a faster-desorbing chlorine ion fragment (HCl^+) correlates well with OA, the difference signal of a slower-desorbing ion fragment (Cl^+) anti-correlates with OA (Fig. S7). The background Cl^+ signal was consistently higher than the sample Cl^+ signal, except when the sample organochloride concentration increased much faster than background, as it does during the SOA formation period in initial Cl_2 injection experiments. Outside the initial SOA formation period, difference Cl^+ signals were negative and difference HCl^+ signals were positive, the summation of which resulted in the low apparent particulate chlorine concentrations.

Low abundance has been cited as the reason for highly variable measurements of ambient particulate chlorine using ACSM and similar instruments (Crenn et al., 2015). Overall, our results indicate that the standard operating procedure of the ACSM and similar instrumentation may systematically underestimate particulate chlorine concentration. To better quantify particulate chlorine, the filtered measurement period could be extended to better capture the true background. Higher vaporizer temperatures could be applied to desorb low-volatility species more efficiently, but doing so could also change the fragmentation profile of all aerosol components. Another approach would be to only use fast-desorbing ions (HCl^+) for quantification: for SOA from chlorine-initiated oxidation of isoprene under low-NO_x conditions, the average HCl^+-to-organics ratio was 0.07 ± 0.01 (Fig. S8).

3.3 SOA yield

It is customary to present SOA yield as a function of OA loading. From Eq. (4), when the VOC precursor is depleted, all subsequent yield Y varies linearly with C_{OA} along a slope

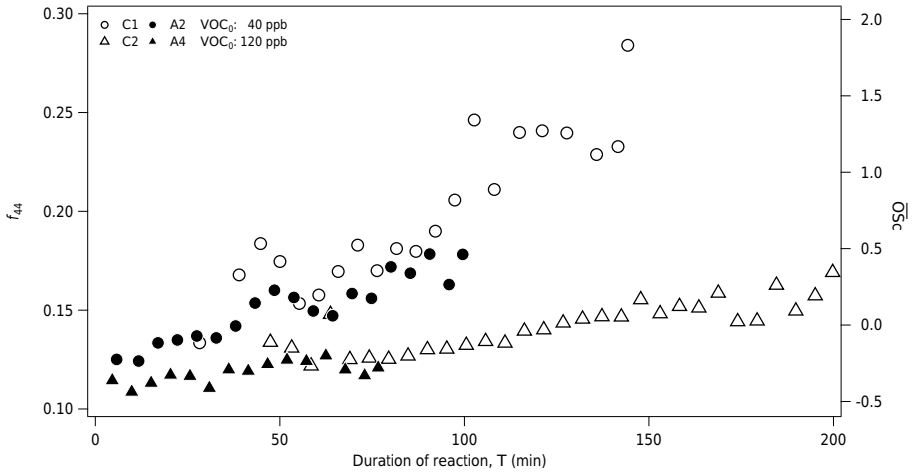

Figure 2. Comparison of SOA aging between two pairs (C1 and A2; C2 and A4) of initial and continuous Cl_2 injection experiments. The trend of f_{44} is consistent for each pair, regardless of chlorine injection method used. Higher initial isoprene concentration resulted in less oxidized organic aerosol (lower f_{44}). $\overline{OS}_C$ is estimated based on f_{44} (see Sect. S2).

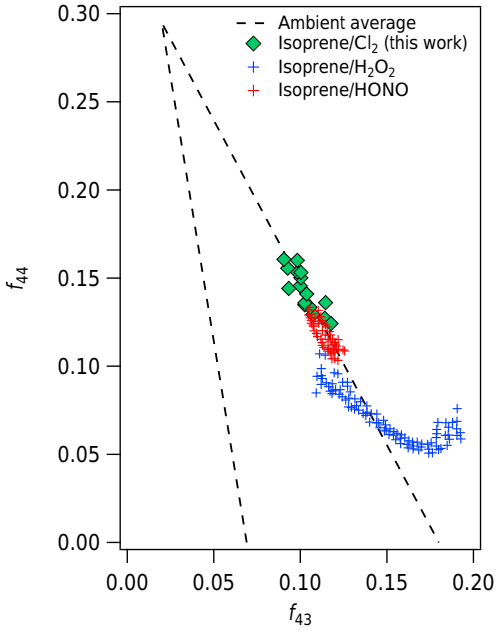

Figure 3. Extent of oxidation of SOA generated from chlorine-initiated reactions (Exp. C3, 5 min averages) compared to OH oxidation of isoprene under low- and high-NO_x conditions (Chhabra et al., 2011). Area enclosed by the dashed lines represent typical ambient OA measurements (Ng et al., 2010).

of $(\Delta VOC_0)^{-1}$, the inverse of the initial VOC concentration. Post VOC depletion, SOA mass may further increase as multi-generational oxidation products partition to the particle phase, but SOA mass will eventually decrease due to fragmentation (Kroll et al., 2011). In theory, all VOC–oxidant mixtures whose ΔVOC_{min} is less than VOC_0 eventually fall somewhere on the same, pre-defined yield "line" with a slope of $(\Delta VOC_0)^{-1}$, and will converge (to Cartesian origin) over time as fragmentation continues. This pre-defined yield curve is thus non-unique and depends only on VOC_0. Incorporating data collected after VOC depletion, whether from the same experiment or different experiments with similar initial VOC_0 values, biases the VBS fitting parameters towards the pre-defined yield curve (see Sect. S5). Therefore, one-dimensional VBS fitting is not sufficient to describe SOA formation and oxidation post VOC depletion, as previous studies have noted (Kroll et al., 2007; Liu et al., 2016; Xu et al., 2014). Two-dimensional modeling would be more appropriate in these cases (Chuang and Donahue, 2016; Donahue et al., 2012; Murphy et al., 2012) but was not performed on this data set.

Complete isoprene depletion, which coincides with the maximum SOA concentration (see Fig. 1), is used as the reference condition for yield reporting in Table 1. Due to uncertainties with organochloride quantification, the particulate chlorine content was not included in the SOA yield calculation. Only results from neutral seed experiments are used for comparison with other literature values of OH oxidation under low- and high-NO_x scenarios (Brégonzio-Rozier et al., 2015; Koo et al., 2014; Liu et al., 2016; Xu et al., 2014) in Fig. 5. In initial Cl_2 injection experiments, maximum SOA concentrations were reached within 15 min, and the effects of vapor wall loss, oxidative fragmentation, and photolysis on reported maximum SOA yields were lower than during continuous Cl_2 injection experiments. Observed SOA yields averaged 20 ± 3 % for initial Cl_2 injection cases (A1–A5) and 8 ± 1 % for continuous Cl_2 injection cases (C1–C4). Under atmospheric conditions, the isoprene-to-chlorine ratio will usually be higher than ratios used in these experiments (0.5–1.2). Previous studies on chlorine-initiated SOA formation from toluene (Cai et al., 2008) and limonene (Cai and Griffin,

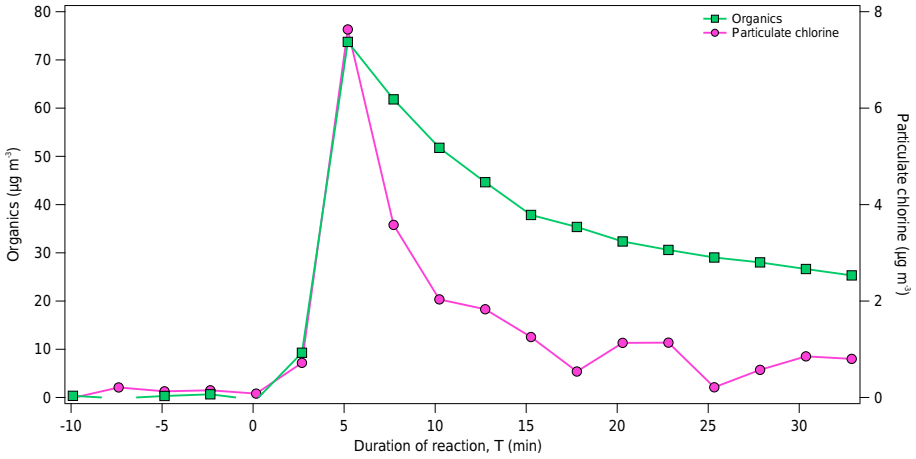

Figure 4. Measurements of particulate organics and chlorine from Exp. A8, not corrected for wall losses. UV was turned on at $T = 0$ mins. Apparent particulate chlorine concentration rapidly decreased to near-background levels while significant suspended OA mass remained. This rapid decrease is likely a measurement artifact due to build-up of chlorinated compounds on the vaporizer surface; see Sects. 3.2 and S4.

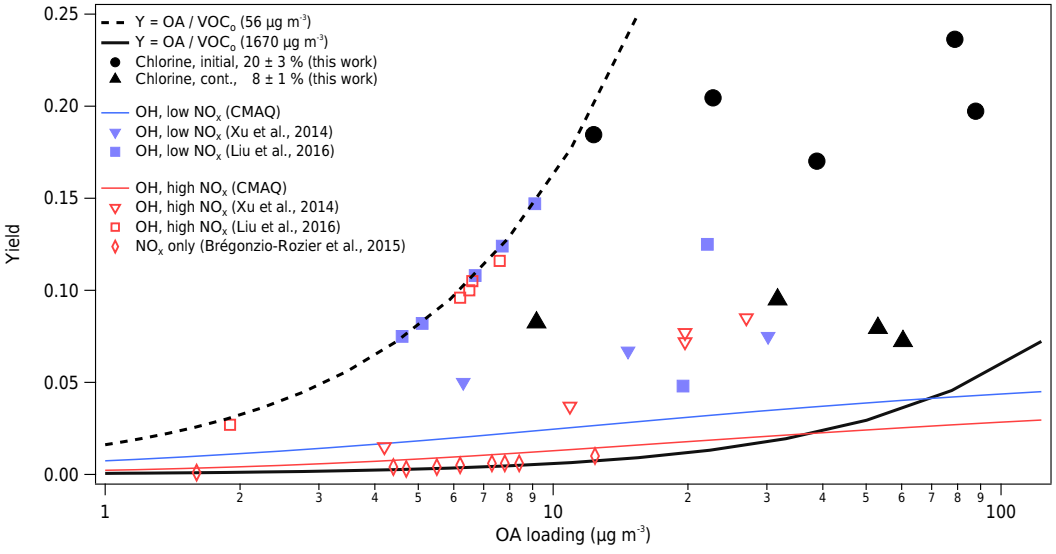

Figure 5. Comparison of observed isoprene–chlorine SOA yield with recent literature values corresponding to low- and high-NO_x OH oxidation. Dashed lines illustrate the concept of a "pre-defined" yield curve as discussed in the text. The yield used in the CMAQ model was reproduced using cited VBS parameters (Koo et al., 2014).

2006) suggest that SOA yields decrease with a higher VOC-to-chlorine ratio. While we did not observe a clear correlation between SOA yield and isoprene-to-chlorine ratios used here (0.5–1.2), such dependence could be present over a wider ratio range. For air quality models which do not explicitly account for fragmentation reactions, the use of the average continuous case yield (8 ± 1 %), which is similar to recently reported OH oxidation yields (Liu et al., 2016; Xu et al., 2014), is more appropriate because the isoprene-to-chlorine ratio is closer to atmospheric conditions and because the SOA yields from continuous injection experiments account for effects of OA aging in the atmosphere (which occur throughout the experiments). The presence of acidic aerosols and inclusion of particulate chlorine content would increase expected yields.

3.4 Gas-phase products: multi-generational oxidation, organochloride formation and secondary OH chemistry

Using $(H_2O)_nH_3O^+$ CIMS, we observed ions consistent with isoprene ($C_5H_8^+$ and $(C_5H_8)H^+$), MACR/MVK ($(C_4H_6O)H^+$), isomers of CMBO ($(C_5H_7ClO)H^+$), 2-methyl-3-buten-2-ol (MBO) ($(C_5H_6O)H^+$), chloroacetone ($(C_3H_5ClO)H^+$), and other gas-phase oxidation products, as shown in Fig. 6a. CMBO, MBO, and MVK/MACR

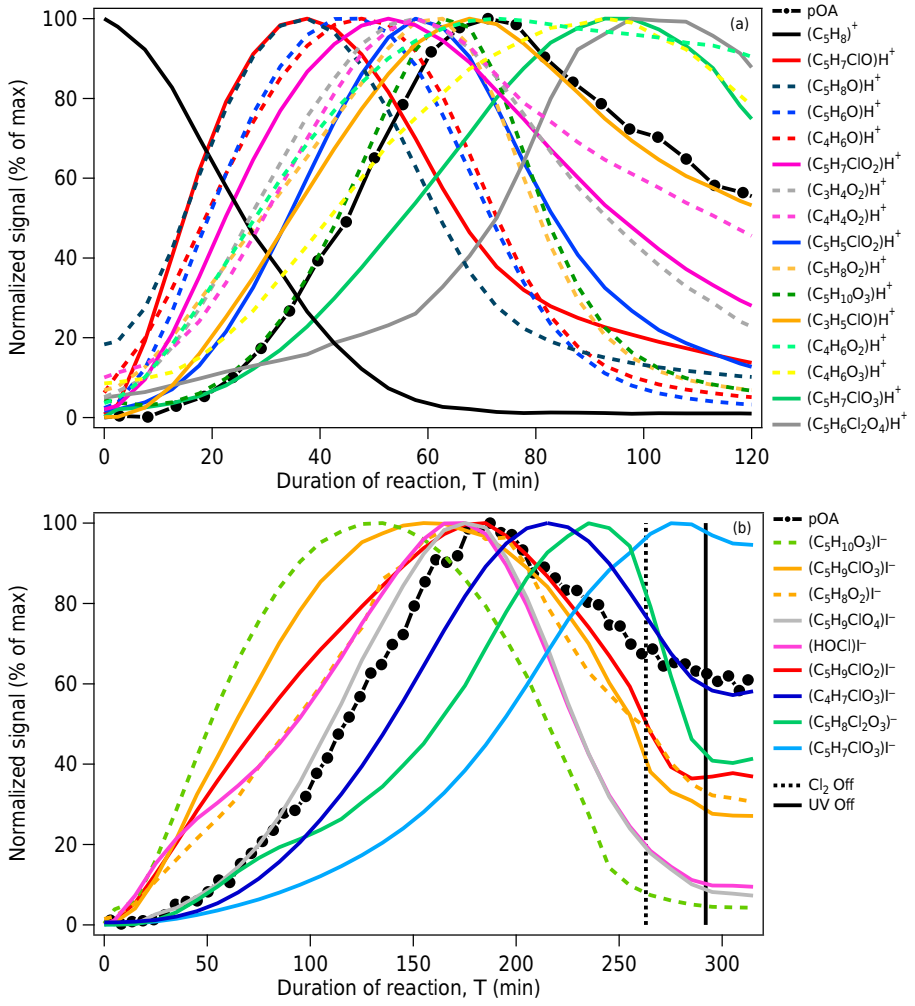

Figure 6. Observation of gas-phase species **(a)** using $(H_2O)_nH_3O^+$ CIMS from Exp. C5 and **(b)** using $(H_2O)_nI^-$ CIMS from Exp. C3. Suspended particle concentration from each experiment is shown. Ion signal for each individual species was normalized to its maximum value. Five-minute averages are shown. Chlorine injection stopped at $T = 263$ min and UV lights were turned off at $T = 292$ min during Exp. C3. Species displayed consist of previously reported products in literatures and multi-generational products proposed in Fig. 7. $(C_5H_{10}O_3)I^-$ potentially represents ISOPOOH or IEPOX, while $(C_5H_{10}O_3)H^+$ is likely $(C_5H_8O_2)(H_3O)^+$, an oxidation product. $(C_4H_7ClO_3)I^-$ may also represent $(C_4H_5ClO_2)(H_2OI)^-$.

were among the earliest oxidation products, which were further oxidized to produce SOA. MVK and MACR are also key intermediary products in OH–isoprene reactions from $NO + RO_2$ and $RO_2 + RO_2$ reaction pathways, where MACR is a known SOA precursor (Brégonzio-Rozier et al., 2015; Kroll et al., 2006; Surratt et al., 2006; Xu et al., 2014), which could contribute to some similarities between OH–isoprene and chlorine–isoprene SOA. Multiple generations of chlorinated C_5 compounds were observed in the gas phase, as shown in Fig. 6a and b, possibly from continued oxidation of CMBO and MBO. Another gas-phase product, C_5H_8O also appeared to act as a SOA precursor, and ions resembling its oxidation products (e.g., $C_5H_7ClO_2$ and $C_5H_9ClO_3$) were observed (see Fig. S12). The formation of C_5H_8O from chlorine–isoprene oxidation has been proposed in the literature (Nordmeyer et al., 1997). Previous studies that observed C_5H_8O during OH-initiated oxidation of isoprene identified it as 2-methylbut-3-enal, but its formation mechanism remains unclear (Brégonzio-Rozier et al., 2015; Healy et al., 2008) and is beyond the scope of this work. It should be noted that CMBO has long been identified as a unique gas-phase marker for isoprene–chlorine oxidation (Chang and Allen, 2006; Nordmeyer et al., 1997; Riemer et al., 2008; Tanaka et al., 2003). Degradation of CMBO by OH is implemented in some air quality models, though only with inferred reaction rates (Tanaka and Allen, 2001). Our gas-phase measurements and proposed reaction products suggest that CMBO undergoes further oxidation reactions initiated by chlorine.

This degradation of CMBO, and its role as a potential SOA precursor, could have important implications for estimating atmospheric chlorine activity and warrants further investigation.

The formation of CMBO and MBO produces HO_2 radicals (Orlando et al., 2003; Ragains and Finlayson-Pitts, 1997), which serve as a source of secondary OH radicals. Other $RO_2 + RO_2$ reaction pathways also produce HO_x radicals. Evidence of secondary OH radical production has been reported for NO_3 oxidation of isoprene (Kwan et al., 2012; Schwantes et al., 2015), for chlorine-initiated oxidation of methylnaphthalenes and naphthalene under low-NO_x conditions (Riva et al., 2015; Wang et al., 2005), and for chlorine-initiated oxidation of toluene under high NO_x (Huang et al., 2012). Figure 6b shows the accumulation of HOCl observed using $(H_2O)_nI^-$ CIMS during the SOA growth period, where HO_x radicals produced from chlorine–isoprene oxidation could react with excess chlorine. Production of OH is also possible from reactions between NO and HO_2 radicals, which would be more pronounced under high-NO_x conditions. No NO_x was added to our experiments, and measured concentrations were below 5 ppb, mostly in the form of NO_2, which may have been released from the Teflon® surface under UV. We use the SOA trend as a common reference because isoprene is not detected using $(H_2O)_nI^-$ CIMS. It can be seen in Figs. 1 and 6a that isoprene depletion roughly coincides with the SOA concentration peak. This explains the reversal from HOCl production to HOCl decay following the SOA concentration peak shown in Fig. 6b, when HO_x radical production from isoprene–chlorine oxidation (e.g., formation of CMBO and MBO) ceased due to isoprene depletion. Accumulated HOCl was then gradually photolyzed under UV. In the absence of a primary oxidant source, such as when chlorine injection stopped in Exp. C3, HOCl could provide residual OH and chlorine radicals under UV. Under dark, dry, and low-NO_x conditions, HOCl remains stable as a temporary radical reservoir, as shown in Fig. 6b during the period when UV lights were turned off.

Secondary OH chemistry also may have contributed to SOA formation. For instance, the $C_5H_8ClO_2^{\bullet}$ radical produced via chlorine addition to isoprene could either undergo $RO_2 + RO_2$ chemistry to produce C_5H_7ClO (e.g., CMBO) or undergo $RO_2 + HO_2$ chemistry to produce $C_5H_9ClO_2$, a chloroalkyl hydroperoxide. Similarly, the $C_5H_7O_2^{\bullet}$ radical produced via hydrogen abstraction from isoprene could either undergo $RO_2 + RO_2$ chemistry to produce C_5H_6O (e.g., MBO) or undergo $RO_2 + HO_2$ chemistry to produce $C_5H_8O_2$, a hydroperoxide. Ions consistent with $C_5H_9ClO_2$ and $C_5H_8O_2$ were observed in the gas phase, as shown in Fig. 6a and b, where the formation of $RO_2 + HO_2$ reaction products appeared delayed compared to their $RO_2 + RO_2$ pathway counterparts. This is consistent with $RO_2 + RO_2$ reactions being a source of HO_x radicals. Figure 7 summarizes select observed gas-phase products whose time series are shown in Fig. 6a and b. More detailed reaction pathways and time series comparisons are shown in Figs. S10–12 in Sect. S6. In the OH–isoprene system, multifunctional, low-volatility hydroperoxides produced from non-IEPOX ("isoprene-derived epoxydiol") reaction pathways contribute to SOA formation under low-NO_x conditions (Krechmer et al., 2015; Liu et al., 2016; Riva et al., 2016). Analogously, in the Cl–isoprene system, the (chloroalkyl) hydroperoxide species identified in Figs. 6 and 7 are expected to contribute to SOA formation.

The ion consistent with isoprene-derived hydroxyl hydroperoxides (ISOPOOH) or IEPOX, $C_5H_{10}O_3$, was observed in $(H_2O)_nI^-$ CIMS, as shown in Fig. 6b. Reactive uptake and oxidation of IEPOX has been reported to contribute significantly to SOA mass during isoprene OH oxidation, especially under acidic or humid conditions (Bates et al., 2014; Gaston et al., 2014; Lewandowski et al., 2015; Lin et al., 2012; Nguyen et al., 2014; Paulot et al., 2009; Surratt et al., 2010). For chlorine-initiated oxidation of isoprene, the SAPRC chamber model results indicate that over 99 % of the isoprene reacts with chlorine; OH oxidation of isoprene is therefore only a very minor pathway in these experiments. Model results also show that HO_2 production is dominated by isoprene–chlorine chemistry when sufficient isoprene is present, whereas wall effects dominate HO_2 production (> 60 %) after all isoprene has been consumed. The model does not explicitly represent chlorine-initiated oxidation of reaction products, which can produce additional HO_x radicals, and therefore likely underestimates the importance of secondary OH chemistry. Furthermore, we note that the observed $(C_5H_{10}O_3)H^+$ and $(C_5H_{10}O_3)I^-$ do not necessarily correspond to ISOPOOH or IEPOX. For instance, whereas $(C_5H_{10}O_3)H^+$ in Fig. 6a trended with $(C_5H_8O_2)H^+$ during SOA growth, $(C_5H_{10}O_3)I^-$ in Fig. 6b appeared early on as an SOA precursor and exhibited a different qualitative trend than $(C_5H_8O_2)I^-$. We can therefore infer that $(C_5H_{10}O_3)H^+$ is an ion cluster in the form of $(C_5H_8O_2)(H_3O)^+$. Without any information on the chemical structure, we surmise that it is also possible that $(C_5H_{10}O_3)I^-$ is the fragment of some unidentified parent ion(s) or that it is an IEPOX isomer produced from non-OH-reaction pathways. Moreover, photooxidative degradation of chlorinated organic compounds could produce products that resemble OH oxidation products like $C_5H_{10}O_3$. A similar observation has been reported for chlorine-initiated oxidation of α-pinene, where the SOA appeared less like halogenated organic aerosol as oxidation continued (Ofner et al., 2013).

Another way to test the presence of IEPOX is to reduce aerosol pH, which should lead to increased uptake of IEPOX (Budisulistiorini et al., 2013; Gaston et al., 2014; Hu et al., 2015; Lin et al., 2012; Riedel et al., 2015, 2016). Comparison of ACSM mass spectra (see Fig. S13) suggests that the presence of acidic aerosol increases the contribution of ion mass fragments at m/z 82 ($C_5H_6O^+$, "f_{82}") to the overall SOA mass, which is associated with IEPOX-derived OA (Budisulistiorini et al., 2013; Hu et al., 2015). However, the

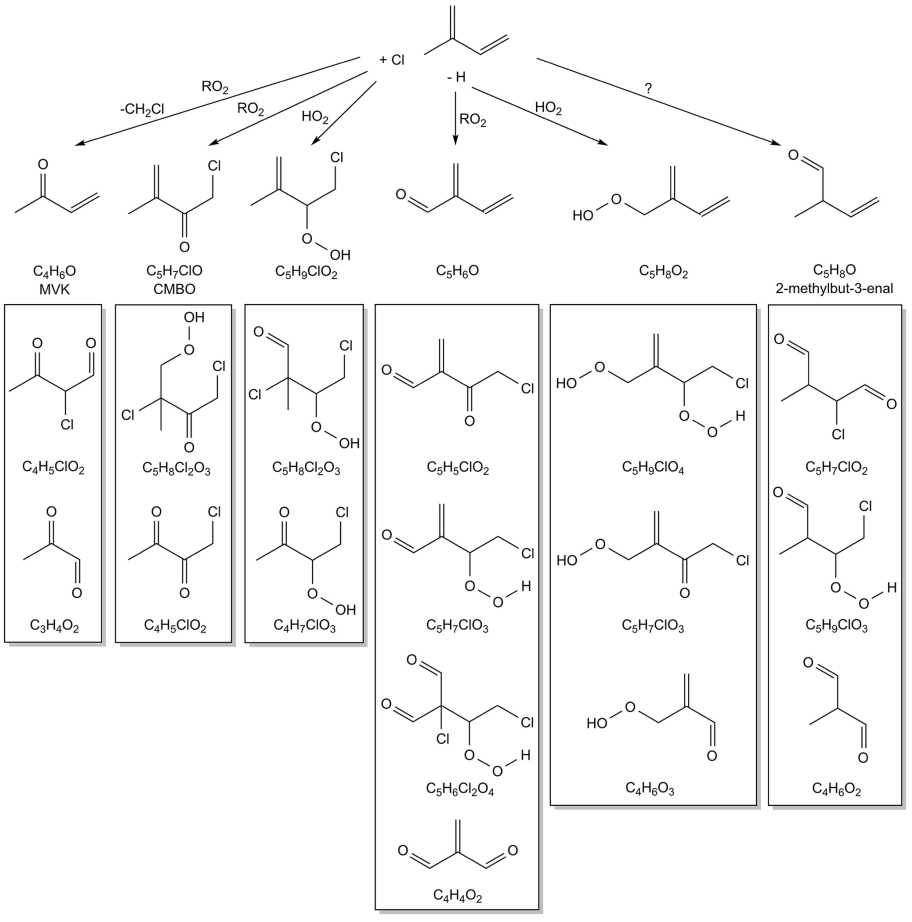

Figure 7. Select oxidation products formed under NO_x-free conditions. More detailed individual reaction pathways are shown in Figs. S10–12. For illustrative purposes, only one isomer is shown per reaction pathway type (e.g., H abstraction vs. Cl addition; $RO_2 + RO_2$ vs. $RO_2 + HO_2$; C-C cleavage vs. no cleavage). As explained in the text, HO_2 radicals required for certain reaction pathways were produced from preceding $RO_2 + RO_2$ chemistry; formation mechanism for C_5H_8O is unclear. Time series of all products shown can be found in either Fig. 6a or b.

magnitude of change is low (1 ‰) and within uncertainty of the instrument. Interference by non-IEPOX-derived OA fragments and non-$C_5H_6O^+$ ions at m/z 82 is also possible. Separate monoterpene–chlorine experiments observed f_{82} values as high as 5 ‰. The observed f_{82} values for isoprene–chlorine SOA are below the average value observed for ambient OA influenced by isoprene emission (6.5 ± 2.2 ‰) and much lower than IEPOX-derived SOA (12–40 ‰) observed in laboratory studies (Hu et al., 2015). We also attempted but were unable to extract an IEPOX factor using positive matrix factorization (Ulbrich et al., 2009), as some studies have done (Budisulistiorini et al., 2013; Lin et al., 2012). Reduction in gas-phase products including those resembling IEPOX was also observed in the CIMS when the aerosol was acidic (see Fig. S14). These observations are consistent with increased partitioning of gas-phase products to the aerosol when the seed aerosol is acidic, resulting in the higher SOA concentrations shown in Fig. 1 and Table 1, but do not prove the presence of IEPOX-derived SOA. Nevertheless, it is clear that SOA formation from chlorine-initiated and OH-initiated oxidation of isoprene proceeds via multi-generational oxidation chemistries involving similar, if not identical, key gas-phase products such as MACR and multifunctional hydroperoxide compounds.

4 Conclusions

Chlorine-initiated oxidation of isoprene under low-NO_x conditions was investigated inside an environmental chamber. Chlorine was injected either in bulk or continuously in low amounts to simulate fast and slower oxidation conditions. Prompt SOA formation was observed in both cases, indicative of the initial formation of low-volatility products. The average wall-loss-corrected SOA yield was 8 ± 1 % for continuous chlorine injection experiments and 20 ± 3 % for initial injection experiments; the differences likely resulted

from a combination of organic vapor wall loss, oxidative fragmentation, and photolysis of SOA. For air quality models which do not explicitly account for SOA aging, the averaged SOA yield from continuous chlorine injection experiments (8 %) should be used for SOA formation from chlorine-initiated oxidation of isoprene. The presence of acidified seed aerosol is shown to enhance SOA formation under low-RH conditions. The extent of oxidation of SOA from chlorine-initiated oxidation of isoprene was similar to that of SOA formed from OH oxidation of isoprene under high-NO_x conditions. CIMS measurements identified several initial gas-phase oxidation products as potential SOA precursors including C_5H_6O (MBO), C_5H_8O (2-methylbut-3-enal), C_5H_7ClO (CMBO), and C_4H_6O (MVK/MACR). Gas-phase data provide evidence of chlorine-initiated secondary OH chemistry and its potential contribution to SOA formation. Ions consistent with hydroperoxides and chloroalkyl hydroperoxides were observed in the CIMS and corresponding HO_x-enabled formation pathways are proposed.

SOA formation from chlorine-initiated oxidation of isoprene is reported for the first time. The high isoprene–chlorine SOA yields suggest that, despite comparatively low ambient abundance, chlorine radicals could have a notable contribution to overall SOA formation. Proposed formation pathways and gas-phase measurements by the CIMS show that chlorine-initiated oxidation of isoprene could produce chloroalkyl hydroperoxide species, analogous to the formation of low-volatility hydroperoxides observed for OH–isoprene oxidation under low-NO_x conditions. These may contribute to the high observed yields, as well as the relatively fast reduction of organic aerosol mass under UV. Challenges associated with the detection and quantification of particulate organochlorides suggest that the prevalence of ambient particulate chlorine is likely underestimated. Overall, our findings indicate that tropospheric chlorine chemistry increases the oxidative capacity of the atmosphere and directly contributes to SOA formation.

Data availability. Data published in this paper's figures and tables are available via the Texas Data Repository, https://doi.org/10.18738/T8/DVALR9 (Wang and Hildebrandt Ruiz, 2017). Underlying research data are also available by request to Lea Hildebrandt Ruiz: lhr@che.utexas.edu.

The Supplement related to this article is available online at https://doi.org/10.5194/acp-17-13491-2017-supplement.

Competing interests. The authors declare that they have no conflict of interest.

Acknowledgements. This material is based upon work supported by the Welch Foundation under grant no. F-1925 and the National Science Foundation under grant no. 1653625. The work was also funded in part with funds from the State of Texas as part of the program of the Texas Air Research Center. The contents do not necessarily reflect the views and policies of the sponsor, nor does the mention of trade names or commercial products constitute endorsement or recommendation for use.

Edited by: Hinrich Grothe
Reviewed by: four anonymous referees

References

Aljawhary, D., Lee, A. K. Y., and Abbatt, J. P. D.: High-resolution chemical ionization mass spectrometry (ToF-CIMS): application to study SOA composition and processing, Atmos. Meas. Tech., 6, 3211–3224, https://doi.org/10.5194/amt-6-3211-2013, 2013.

Allan, J. D., Delia, A. E., Coe, H., Bower, K. N., Alfarra, M. R., Jimenez, J. L., Middlebrook, A. M., Drewnick, F., Onasch, T. B., Canagaratna, M. R., Jayne, J. T., and Worsnop, D. R.: A generalised method for the extraction of chemically resolved mass spectra from Aerodyne aerosol mass spectrometer data, J. Aerosol Sci., 35, 909–922, https://doi.org/10.1016/j.jaerosci.2004.02.007, 2004.

Arnold, S. R., Spracklen, D. V., Williams, J., Yassaa, N., Sciare, J., Bonsang, B., Gros, V., Peeken, I., Lewis, A. C., Alvain, S., and Moulin, C.: Evaluation of the global oceanic isoprene source and its impacts on marine organic carbon aerosol, Atmos. Chem. Phys., 9, 1253–1262, https://doi.org/10.5194/acp-9-1253-2009, 2009.

Atkinson, R. and Arey, J.: Atmospheric degradation of volatile organic compounds, Chem. Rev., 103, 4605–4638, https://doi.org/10.1021/cr0206420, 2003.

Bates, K. H., Crounse, J. D., St. Clair, J. M., Bennett, N. B., Nguyen, T. B., Seinfeld, J. H., Stoltz, B. M., and Wennberg, P. O.: Gas phase production and loss of isoprene epoxydiols, J. Phys. Chem. A, 118, 1237–1246, https://doi.org/10.1021/jp4107958, 2014.

Bean, J. K. and Hildebrandt Ruiz, L.: Gas–particle partitioning and hydrolysis of organic nitrates formed from the oxidation of α-pinene in environmental chamber experiments, Atmos. Chem. Phys., 16, 2175–2184, https://doi.org/10.5194/acp-16-2175-2016, 2016.

Bertram, T. H., Kimmel, J. R., Crisp, T. A., Ryder, O. S., Yatavelli, R. L. N., Thornton, J. A., Cubison, M. J., Gonin, M., and Worsnop, D. R.: A field-deployable, chemical ionization time-of-flight mass spectrometer, Atmos. Meas. Tech., 4, 1471–1479, https://doi.org/10.5194/amt-4-1471-2011, 2011.

Bikkina, S., Kawamura, K., Miyazaki, Y., and Fu, P.: High abundances of oxalic, azelaic, and glyoxylic acids and methylglyoxal in the open ocean with high biological activity: Implication for secondary OA formation from isoprene, Geophys. Res. Lett., 41, 3649–3657, https://doi.org/10.1002/2014GL059913, 2014.

Bobrowski, N., von Glasow, R., Aiuppa, A., Inguaggiato, S., Louban, I., Ibrahim, O. W., and Platt, U.: Reactive halogen chemistry in volcanic plumes, J. Geophys. Res.-Atmos., 112, 1–17, https://doi.org/10.1029/2006JD007206, 2007.

Boyd, C. M., Sanchez, J., Xu, L., Eugene, A. J., Nah, T., Tuet, W. Y., Guzman, M. I., and Ng, N. L.: Secondary organic aerosol formation from the β-pinene+NO_3 system: effect of humidity and peroxy radical fate, Atmos. Chem. Phys., 15, 7497–7522, https://doi.org/10.5194/acp-15-7497-2015, 2015.

Brégonzio-Rozier, L., Siekmann, F., Giorio, C., Pangui, E., Morales, S. B., Temime-Roussel, B., Gratien, A., Michoud, V., Ravier, S., Cazaunau, M., Tapparo, A., Monod, A., and Doussin, J.-F.: Gaseous products and secondary organic aerosol formation during long term oxidation of isoprene and methacrolein, Atmos. Chem. Phys., 15, 2953–2968, https://doi.org/10.5194/acp-15-2953-2015, 2015.

Budisulistiorini, S. H., Canagaratna, M. R., Croteau, P. L., Marth, W. J., Baumann, K., Edgerton, E. S., Shaw, S. L., Knipping, E. M., Worsnop, D. R., Jayne, J. T., Gold, A., and Surratt, J. D.: Real-time continuous characterization of secondary organic aerosol derived from isoprene epoxydiols in downtown Atlanta, Georgia, using the aerodyne aerosol chemical speciation monitor, Environ. Sci. Technol., 47, 5686–5694, https://doi.org/10.1021/es400023n, 2013.

Buxmann, J., Bleicher, S., Platt, U., von Glasow, R., Sommariva, R., Held, A., Zetzsch, C., and Ofner, J.: Consumption of reactive halogen species from sea-salt aerosol by secondary organic aerosol: slowing down the bromine explosion, Environ. Chem., 12, 476, https://doi.org/10.1071/EN14226, 2015.

Buys, Z., Brough, N., Huey, L. G., Tanner, D. J., von Glasow, R., and Jones, A. E.: High temporal resolution Br_2, BrCl and BrO observations in coastal Antarctica, Atmos. Chem. Phys., 13, 1329–1343, https://doi.org/10.5194/acp-13-1329-2013, 2013.

Cai, X. and Griffin, R. J.: Secondary aerosol formation from the oxidation of biogenic hydrocarbons by chlorine atoms, J. Geophys. Res.-Atmos., 111, 7348–7359, https://doi.org/10.1029/2005JD006857, 2006.

Cai, X., Ziemba, L. D., and Griffin, R. J.: Secondary aerosol formation from the oxidation of toluene by chlorine atoms, Atmos. Environ., 42, 7348–7359, https://doi.org/10.1016/j.atmosenv.2008.07.014, 2008.

Canagaratna, M. R., Jimenez, J. L., Kroll, J. H., Chen, Q., Kessler, S. H., Massoli, P., Hildebrandt Ruiz, L., Fortner, E., Williams, L. R., Wilson, K. R., Surratt, J. D., Donahue, N. M., Jayne, J. T., and Worsnop, D. R.: Elemental ratio measurements of organic compounds using aerosol mass spectrometry: characterization, improved calibration, and implications, Atmos. Chem. Phys., 15, 253–272, https://doi.org/10.5194/acp-15-253-2015, 2015.

Carter, W. P. L., Cocker, D. R., Fitz, D. R., Malkina, I. L., Bumiller, K., Sauer, C. G., Pisano, J. T., Bufalino, C., and Song, C.: A new environmental chamber for evaluation of gas-phase chemical mechanisms and secondary aerosol formation, Atmos. Environ., 39, 7768–7788, https://doi.org/10.1016/j.atmosenv.2005.08.040, 2005.

Chan, M. N., Surratt, J. D., Claeys, M., Edgerton, E. S., Tanner, R. L., Shaw, S. L., Zheng, M., Knipping, E. M., Eddingsaas, N. C., Wennberg, P. O., and Seinfeld, J. H.: Characterization and quantification of isoprene-derived epoxydiols in ambient aerosol in the southeastern united states, Environ. Sci. Technol., 44, 4590–4596, https://doi.org/10.1021/es100596b, 2010.

Chang, S. and Allen, D. T.: Atmospheric chlorine chemistry in southeast Texas: Impacts on ozone formation and control, Environ. Sci. Technol., 40, 251–262, https://doi.org/10.1007/s10479-006-0033-8, 2006.

Chang, S., Tanaka, P., Mcdonald-buller, E., and Allen, D. T.: Emission inventory for atomic chlorine precursors in Southeast Texas, Rep. Contract 9880077600-18 between Univ. Texas and Texas Nat. Resour. Conserv. Comm., available at: https://www.tceq.texas.gov/assets/public/implementation/air/am/contracts/reports/oth/EmissioninventoryForAtomicChlorinePrecursors.pdf (last access: 4 October 2017), 1–27, 2001.

Chhabra, P. S., Ng, N. L., Canagaratna, M. R., Corrigan, A. L., Russell, L. M., Worsnop, D. R., Flagan, R. C., and Seinfeld, J. H.: Elemental composition and oxidation of chamber organic aerosol, Atmos. Chem. Phys., 11, 8827–8845, https://doi.org/10.5194/acp-11-8827-2011, 2011.

Chuang, W. K. and Donahue, N. M.: A two-dimensional volatility basis set – Part 3: Prognostic modeling and NOx dependence, Atmos. Chem. Phys., 16, 123–134, https://doi.org/10.5194/acp-16-123-2016, 2016.

Claeys, M.: Formation of Secondary Organic Aerosols Through Photooxidation of Isoprene, Science, 303, 1173–1176, https://doi.org/10.1126/science.1092805, 2004.

Crenn, V., Sciare, J., Croteau, P. L., Verlhac, S., Fröhlich, R., Belis, C. A., Aas, W., Äijälä, M., Alastuey, A., Artiñano, B., Baisnée, D., Bonnaire, N., Bressi, M., Canagaratna, M., Canonaco, F., Carbone, C., Cavalli, F., Coz, E., Cubison, M. J., Esser-Gietl, J. K., Green, D. C., Gros, V., Heikkinen, L., Herrmann, H., Lunder, C., Minguillón, M. C., Mocnik, G., O'Dowd, C. D., Ovadnevaite, J., Petit, J.-E., Petralia, E., Poulain, L., Priestman, M., Riffault, V., Ripoll, A., Sarda-Estève, R., Slowik, J. G., Setyan, A., Wiedensohler, A., Baltensperger, U., Prévôt, A. S. H., Jayne, J. T., and Favez, O.: ACTRIS ACSM intercomparison – Part 1: Reproducibility of concentration and fragment results from 13 individual Quadrupole Aerosol Chemical Speciation Monitors (Q-ACSM) and consistency with co-located instruments, Atmos. Meas. Tech., 8, 5063–5087, https://doi.org/10.5194/amt-8-5063-2015, 2015.

Crutzen, P.: A review of upper atmospheric photochemistry, Can. J. Chem., 52, 1569–1581, https://doi.org/10.1139/v74-229, 1974.

de Bruijne, K., Ebersviller, S., Sexton, K. G., Lake, S., Leith, D., Goodman, R., Jetters, J., Walters, G. W., Doyle-Eisele, M., Woodside, R., Jeffries, H. E., and Jaspers, I.: Design and testing of Electrostatic Aerosol in Vitro Exposure System (EAVES): an alternative exposure system for particles., Inhal. Toxicol., 21, 91–101, https://doi.org/10.1080/08958370802166035, 2009.

de Gouw, J. and Warneke, C.: Measurements of volatile organic compounds in the earth's atmosphere using proton-transfer-reaction mass spectrometry, Mass Spectrom. Rev., 26, 223–257, https://doi.org/10.1002/mas.20119, 2007.

Dockery, D. W., Pope, C. A., Xu, X., Spengler, J. D., Ware, J. H., Fay, M. E., Ferris, B. G., and Speizer, F. E.: An association between air pollution and mortality in six U.S. cities, N. Engl. J. Med., 329, 1753–1759, https://doi.org/10.1056/NEJM199312093292401, 1993.

Donahue, N. M., Robinson, A. L., Stanier, C. O., and Pandis, S. N.: Coupled partitioning, dilution, and chemical aging of semivolatile organics, Environ. Sci. Technol., 40, 2635–2643, https://doi.org/10.1021/es052297c, 2006.

Donahue, N. M., Kroll, J. H., Pandis, S. N., and Robinson, A. L.: A two-dimensional volatility basis set – Part 2: Diagnostics of organic-aerosol evolution, Atmos. Chem. Phys., 12, 615–634, https://doi.org/10.5194/acp-12-615-2012, 2012.

Ebersviller, S., Lichtveld, K., Sexton, K. G., Zavala, J., Lin, Y.-H., Jaspers, I., and Jeffries, H. E.: Gaseous VOCs rapidly modify particulate matter and its biological effects – Part 1: Simple VOCs and model PM, Atmos. Chem. Phys., 12, 12277–12292, https://doi.org/10.5194/acp-12-12277-2012, 2012.

Edwards, P. M., Young, C. J., Aikin, K., deGouw, J., Dubé, W. P., Geiger, F., Gilman, J., Helmig, D., Holloway, J. S., Kercher, J., Lerner, B., Martin, R., McLaren, R., Parrish, D. D., Peischl, J., Roberts, J. M., Ryerson, T. B., Thornton, J., Warneke, C., Williams, E. J., and Brown, S. S.: Ozone photochemistry in an oil and natural gas extraction region during winter: simulations of a snow-free season in the Uintah Basin, Utah, Atmos. Chem. Phys., 13, 8955–8971, https://doi.org/10.5194/acp-13-8955-2013, 2013.

Edwards, P. M., Brown, S. S., Roberts, J. M., Ahmadov, R., Banta, R. M., deGouw, J. A., Dube, W. P., Field, R. A., Flynn, J. H., Gilman, J. B., Graus, M., Helmig, D., Koss, A., Langford, A. O., Lefer, B. L., Lerner, B. M., Li, R., Li, S. M., McKeen, S. A., Murphy, S. M., Parrish, D. D., Senff, C. J., Soltis, J., Stutz, J., Sweeney, C., Thompson, C. R., Trainer, M. K., Tsai, C., Veres, P. R., Washenfelder, R. A., Warneke, C., Wild, R. J., Young, C. J., Yuan, B., and Zamora, R.: High winter ozone pollution from carbonyl photolysis in an oil and gas basin, Nature, 514, 351–354, https://doi.org/10.1038/nature13767, 2014.

Fan, J. and Zhang, R.: Atmospheric oxidation mechanism of isoprene, Environ. Chem., 1, 140–149, https://doi.org/10.1071/EN04045, 2004.

Fantechi, G., Jensen, N. R., Saastad, O., Hjorth, J., and Peeters, J.: Reactions of Cl atoms with selected VOCs: Kinetics, products and mechanisms, J. Atmos. Chem., 31, 247–267, https://doi.org/10.1023/A:1006033910014, 1998.

Faxon, C. B. and Allen, D. T.: Chlorine chemistry in urban atmospheres: A review, Environ. Chem., 10, 221–233, https://doi.org/10.1071/EN13026, 2013.

Faxon, C., Bean, J., and Hildebrandt Ruiz, L.: Inland concentrations of Cl_2 and $ClNO_2$ in Southeast Texas suggest chlorine chemistry significantly contributes to atmospheric reactivity, Atmosphere, 6, 1487–1506, https://doi.org/10.3390/atmos6101487, 2015.

Finlayson-Pitts, B. J.: Halogens in the troposphere, Anal. Chem., 82, 770–776, https://doi.org/10.1021/ac901478p, 2010.

Fu, P., Kawamura, K., and Miura, K.: Molecular characterization of marine organic aerosols collected during a round-the-world cruise, J. Geophys. Res.-Atmos., 116, 1–14, https://doi.org/10.1029/2011JD015604, 2011.

Fu, P. Q., Kawamura, K., Chen, J., Charrière, B., and Sempéré, R.: Organic molecular composition of marine aerosols over the Arctic Ocean in summer: contributions of primary emission and secondary aerosol formation, Biogeosciences, 10, 653–667, https://doi.org/10.5194/bg-10-653-2013, 2013.

Gantt, B., Meskhidze, N., Zhang, Y., and Xu, J.: The effect of marine isoprene emissions on secondary organic aerosol and ozone formation in the coastal United States, Atmos. Environ., 44, 115–121, https://doi.org/10.1016/j.atmosenv.2009.08.027, 2010.

Gantt, B., Johnson, M. S., Crippa, M., Prévôt, A. S. H., and Meskhidze, N.: Implementing marine organic aerosols into the GEOS-Chem model, Geosci. Model Dev., 8, 619–629, https://doi.org/10.5194/gmd-8-619-2015, 2015.

Gaston, C. J., Riedel, T. P., Zhang, Z., Gold, A., Surratt, J. D., and Thornton, J. A.: Reactive uptake of an isoprene-derived epoxydiol to submicron aerosol particles, Environ. Sci. Technol., 48, 11178–11186, https://doi.org/10.1021/es5034266, 2014.

Goldstein, A. H. and Galbally, I. E.: Known and unexplored organic constituents in the earth's atmosphere, Environ. Sci. Technol., 41, 1514–1521, https://doi.org/10.1021/es072476p, 2007.

Griffin, R. J., Cocker, D. R., and Seinfeld, J. H.: Incremental aerosol reactivity: Application to aromatic and biogenic hydrocarbons, Environ. Sci. Technol., 33, 2403–2408, https://doi.org/10.1021/es981330a, 1999.

Guenther, A., Karl, T., Harley, P., Wiedinmyer, C., Palmer, P. I., and Geron, C.: Estimates of global terrestrial isoprene emissions using MEGAN (Model of Emissions of Gases and Aerosols from Nature), Atmos. Chem. Phys., 6, 3181–3210, https://doi.org/10.5194/acp-6-3181-2006, 2006.

Guenther, A. B., Jiang, X., Heald, C. L., Sakulyanontvittaya, T., Duhl, T., Emmons, L. K., and Wang, X.: The Model of Emissions of Gases and Aerosols from Nature version 2.1 (MEGAN2.1): an extended and updated framework for modeling biogenic emissions, Geosci. Model Dev., 5, 1471–1492, https://doi.org/10.5194/gmd-5-1471-2012, 2012.

Hawley, B., McKenna, D., Marchese, A., and Volckens, J.: Time course of bronchial cell inflammation following exposure to diesel particulate matter using a modified EAVES, Toxicol. Vitr., 28, 829–837, https://doi.org/10.1016/j.tiv.2014.03.001, 2014.

Heald, C. L., Kroll, J. H., Jimenez, J. L., Docherty, K. S., Decarlo, P. F., Aiken, A. C., Chen, Q., Martin, S. T., Farmer, D. K., and Artaxo, P.: A simplified description of the evolution of organic aerosol composition in the atmosphere, Geophys. Res. Lett., 37, L08803, https://doi.org/10.1029/2010GL042737, 2010.

Healy, R. M., Wenger, J. C., Metzger, A., Duplissy, J., Kalberer, M., and Dommen, J.: Gas/particle partitioning of carbonyls in the photooxidation of isoprene and 1,3,5-trimethylbenzene, Atmos. Chem. Phys., 8, 3215–3230, https://doi.org/10.5194/acp-8-3215-2008, 2008.

Hildebrandt, L., Donahue, N. M., and Pandis, S. N.: High formation of secondary organic aerosol from the photooxidation of toluene, Atmos. Chem. Phys., 9, 2973–2986, https://doi.org/10.5194/acp-9-2973-2009, 2009.

Hu, Q.-H., Xie, Z.-Q., Wang, X.-M., Kang, H., He, Q.-F., and Zhang, P.: Secondary organic aerosols over oceans via oxidation of isoprene and monoterpenes from Arctic to Antarctic, Sci. Rep., 3, 2280, https://doi.org/10.1038/srep02280, 2013.

Hu, W. W., Campuzano-Jost, P., Palm, B. B., Day, D. A., Ortega, A. M., Hayes, P. L., Krechmer, J. E., Chen, Q., Kuwata, M., Liu, Y. J., de Sá, S. S., McKinney, K., Martin, S. T., Hu, M., Budisulistiorini, S. H., Riva, M., Surratt, J. D., St. Clair, J. M., Isaacman-Van Wertz, G., Yee, L. D., Goldstein, A. H., Carbone, S., Brito, J., Artaxo, P., de Gouw, J. A., Koss, A., Wisthaler, A., Mikoviny, T., Karl, T., Kaser, L., Jud, W., Hansel, A., Docherty, K. S., Alexander, M. L., Robinson, N. H., Coe, H., Allan, J. D., Canagaratna, M. R., Paulot, F., and Jimenez, J. L.: Characterization of a real-time tracer for isoprene epoxydiols-derived secondary organic aerosol (IEPOX-SOA) from aerosol mass spectrometer measurements, Atmos. Chem. Phys., 15, 11807–11833, https://doi.org/10.5194/acp-15-11807-2015, 2015.

Huang, M., Zhang, W., Gu, X., Hu, C., Zhao, W., Wang, Z., and Fang, L.: Size distribution and chemical composition of secondary organic aerosol formed from Cl-initiated oxidation of toluene, J. Environ. Sci., 24, 860–864, https://doi.org/10.1016/S1001-0742(11)60840-1, 2012.

Huang, M., Liu, X., Hu, C., Guo, X., Gu, X., Zhao, W., Wang, Z., Fang, L., and Zhang, W.: Aerosol laser time-of-flight mass spectrometer for the on-line measurement of secondary organic aerosol in smog chamber, Meas. J. Int. Meas. Confed., 55, 394–401, https://doi.org/10.1016/j.measurement.2014.05.038, 2014.

Jimenez, J. L., Canagaratna, M. R., Donahue, N. M., Prevot, A. S. H., Zhang, Q., Kroll, J. H., DeCarlo, P. F., Allan, J. D., Coe, H., Ng, N. L., Aiken, A. C., Docherty, K. S., Ulbrich, I. M., Grieshop, A. P., Robinson, A. L., Duplissy, J., Smith, J. D., Wilson, K. R., Lanz, V. A., Hueglin, C., Sun, Y. L., Tian, J., Laaksonen, A., Raatikainen, T., Rautiainen, J., Vaattovaara, P., Ehn, M., Kulmala, M., Tomlinson, J. M., Collins, D. R., Cubison, M. J., Dunlea, J., Huffman, J. A., Onasch, T. B., Alfarra, M. R., Williams, P. I., Bower, K., Kondo, Y., Schneider, J., Drewnick, F., Borrmann, S., Weimer, S., Demerjian, K., Salcedo, D., Cottrell, L., Griffin, R., Takami, A., Miyoshi, T., Hatakeyama, S., Shimono, A., Sun, J. Y., Zhang, Y. M., Dzepina, K., Kimmel, J. R., Sueper, D., Jayne, J. T., Herndon, S. C., Trimborn, A. M., Williams, L. R., Wood, E. C., Middlebrook, A. M., Kolb, C. E., Baltensperger, U., and Worsnop, D. R.: Evolution of organic aerosols in the atmosphere, Science, 326, 1525–1529, https://doi.org/10.1126/science.1180353, 2009.

Kamilli, K. A., Ofner, J., Lendl, B., Schmitt-Kopplin, P., and Held, A.: New particle formation above a simulated salt lake in aerosol chamber experiments, Environ. Chem., 12, 489–503, https://doi.org/10.1071/EN14225, 2015.

Kamilli, K. A., Ofner, J., Krause, T., Sattler, T., Schmitt-Kopplin, P., Eitenberger, E., Friedbacher, G., Lendl, B., Lohninger, H., Schöler, H. F., and Held, A.: How salt lakes affect atmospheric new particle formation: A case study in Western Australia, Sci. Total Environ., 573, 985–995, https://doi.org/10.1016/j.scitotenv.2016.08.058, 2016.

Kanakidou, M., Seinfeld, J. H., Pandis, S. N., Barnes, I., Dentener, F. J., Facchini, M. C., Van Dingenen, R., Ervens, B., Nenes, A., Nielsen, C. J., Swietlicki, E., Putaud, J. P., Balkanski, Y., Fuzzi, S., Horth, J., Moortgat, G. K., Winterhalter, R., Myhre, C. E. L., Tsigaridis, K., Vignati, E., Stephanou, E. G., and Wilson, J.: Organic aerosol and global climate modelling: a review, Atmos. Chem. Phys., 5, 1053–1123, https://doi.org/10.5194/acp-5-1053-2005, 2005.

Karlsson, R. S., Szente, J. J., Ball, J. C., and Maricq, M. M.: Homogeneous aerosol formation by the chlorine atom initiated oxidation of toluene, J. Phys. Chem. A, 105, 82–96, https://doi.org/10.1021/jp001831u, 2001.

Kokkola, H., Yli-Pirilä, P., Vesterinen, M., Korhonen, H., Keskinen, H., Romakkaniemi, S., Hao, L., Kortelainen, A., Joutsensaari, J., Worsnop, D. R., Virtanen, A., and Lehtinen, K. E. J.: The role of low volatile organics on secondary organic aerosol formation, Atmos. Chem. Phys., 14, 1689–1700, https://doi.org/10.5194/acp-14-1689-2014, 2014.

Koo, B., Knipping, E., and Yarwood, G.: 1.5-Dimensional volatility basis set approach for modeling organic aerosol in CAMx and CMAQ, Atmos. Environ., 95, 158–164, https://doi.org/10.1016/j.atmosenv.2014.06.031, 2014.

Krechmer, J. E., Coggon, M. M., Massoli, P., Nguyen, T. B., Crounse, J. D., Hu, W., Day, D. A., Tyndall, G. S., Henze, D. K., Rivera-Rios, J. C., Nowak, J. B., Kimmel, J. R., Mauldin, R. L., Stark, H., Jayne, J. T., Sipila, M., Junninen, H., St. Clair, J. M., Zhang, X., Feiner, P. A., Zhang, L., Miller, D. O., Brune, W. H., Keutsch, F. N., Wennberg, P. O., Seinfeld, J. H., Worsnop, D. R., Jimenez, J. L., and Canagaratna, M. R.: Formation of low volatility organic compounds and secondary organic aerosol from isoprene hydroxyhydroperoxide low-NO oxidation, Environ. Sci. Technol., 49, 10330–10339, https://doi.org/10.1021/acs.est.5b02031, 2015.

Krechmer, J. E., Pagonis, D., Ziemann, P. J., and Jimenez, J. L. L.: Quantification of gas-wall partitioning in Teflon environmental chambers using rapid bursts of low-volatility oxidized species generated in-situ, Environ. Sci. Technol., 50, 5757–5765, https://doi.org/10.1021/acs.est.6b00606, 2016.

Kroll, J. H., Ng, N. L., Murphy, S. M., Flagan, R. C., and Seinfeld, J. H.: Secondary organic aerosol formation from isoprene photooxidation., Environ. Sci. Technol., 40, 1869–1877, https://doi.org/10.1021/es0524301, 2006.

Kroll, J. H., Chan, A. W. H., Ng, N. L., Flagan, R. C., and Seinfeld, J. H.: Reactions of semivolatile organics and their effects on secondary organic aerosol formation, Environ. Sci. Technol., 41, 3545–3550, https://doi.org/10.1021/es062059x, 2007.

Kroll, J. H., Donahue, N. M., Jimenez, J. L., Kessler, S. H., Canagaratna, M. R., Wilson, K. R., Altieri, K. E., Mazzoleni, L. R., Wozniak, A. S., Bluhm, H., Mysak, E. R., Smith, J. D., Kolb, C. E., and Worsnop, D. R.: Carbon oxidation state as a metric for describing the chemistry of atmospheric organic aerosol., Nat. Chem., 3, 133–139, https://doi.org/10.1038/nchem.948, 2011.

Kwan, A. J., Chan, A. W. H., Ng, N. L., Kjaergaard, H. G., Seinfeld, J. H., and Wennberg, P. O.: Peroxy radical chemistry and OH radical production during the NO_3-initiated oxidation of isoprene, Atmos. Chem. Phys., 12, 7499–7515, https://doi.org/10.5194/acp-12-7499-2012, 2012.

Lawler, M. J., Sander, R., Carpenter, L. J., Lee, J. D., von Glasow, R., Sommariva, R., and Saltzman, E. S.: HOCl and Cl_2 observations in marine air, Atmos. Chem. Phys., 11, 7617–7628, https://doi.org/10.5194/acp-11-7617-2011, 2011.

Lee, B. H., Lopez-Hilfiker, F. D., Mohr, C., Kurtén, T., Worsnop, D. R., and Thornton, J. A.: An iodide-adduct high-resolution time-of-flight chemical-ionization mass spectrometer: Application to atmospheric inorganic and organic compounds, Environ. Sci. Technol., 48, 6309–6317, https://doi.org/10.1021/es500362a, 2014.

Lei, W. and Zhang, R.: Chlorine atom addition reaction to isoprene: a theoretical study, J. Chem. Phys., 113, 153–157, https://doi.org/10.1063/1.481782, 2000.

Lewandowski, M., Jaoui, M., Offenberg, J. H., Krug, J. D., and Kleindienst, T. E.: Atmospheric oxidation of isoprene and 1,3-butadiene: influence of aerosol acidity and relative humidity on secondary organic aerosol, Atmos. Chem. Phys., 15, 3773–3783, https://doi.org/10.5194/acp-15-3773-2015, 2015.

Liao, J., Huey, L. G., Liu, Z., Tanner, D. J., Cantrell, C. A., Orlando, J. J., Flocke, F. M., Shepson, P. B., Weinheimer, A. J., Hall, S. R., Ullmann, K., Beine, H. J., Wang, Y., Ingall, E. D., Stephens, C. R., Hornbrook, R. S., Apel, E. C., Riemer, D., Fried, A., Mauldin, R. L., Smith, J. N., Staebler, R. M., Neuman, J. A., and Nowak,

J. B.: High levels of molecular chlorine in the Arctic atmosphere, Nat. Geosci., 7, 91–94, https://doi.org/10.1038/ngeo2046, 2014.

Lin, Y. H., Zhang, Z., Docherty, K. S., Zhang, H., Budisulistiorini, S. H., Rubitschun, C. L., Shaw, S. L., Knipping, E. M., Edgerton, E. S., Kleindienst, T. E., Gold, A., and Surratt, J. D.: Isoprene epoxydiols as precursors to secondary organic aerosol formation: Acid-catalyzed reactive uptake studies with authentic compounds, Environ. Sci. Technol., 46, 250–258, https://doi.org/10.1021/es202554c, 2012.

Liu, J., D'Ambro, E. L., Lee, B. H., Lopez-Hilfiker, F. D., Zaveri, R. A., Rivera-Rios, J. C., Keutsch, F. N., Iyer, S., Kurten, T., Zhang, Z., Gold, A., Surratt, J. D., Shilling, J. E., and Thornton, J. A.: Efficient isoprene secondary prganic aerosol formation from a non-IEPOX pathway, Environ. Sci. Technol., 50, 9872–9880, https://doi.org/10.1021/acs.est.6b01872, 2016.

Lobert, J. M., Keene, W. C., Logan, J. A., and Yevich, R.: Global chlorine emissions from biomass burning: Reactive Chlorine Emissions Inventory, J. Geophys. Res.-Atmos., 104, 8373–8389, https://doi.org/10.1029/1998JD100077, 1999.

Loza, C. L., Chan, A. W. H., Galloway, M. M., Keutsch, F. N., Flagan, R. C., and Seinfeld, J. H.: Characterization of vapor wall loss in laboratory chambers, Environ. Sci. Technol., 44, 5074–5078, https://doi.org/10.1021/es100727v, 2010.

Luo, G. and Yu, F.: A numerical evaluation of global oceanic emissions of α-pinene and isoprene, Atmos. Chem. Phys., 10, 2007–2015, https://doi.org/10.5194/acp-10-2007-2010, 2010.

Matsunaga, A. and Ziemann, P. J.: Gas-Wall Partitioning of Organic Compounds in a Teflon Film Chamber and Potential Effects on Reaction Product and Aerosol Yield Measurements, Aerosol Sci. Technol., 44, 881–892, https://doi.org/10.1080/02786826.2010.501044, 2010.

Mielke, L. H., Stutz, J., Tsai, C., Hurlock, S. C., Roberts, J. M., Veres, P. R., Froyd, K. D., Hayes, P. L., Cubison, M. J., Jimenez, J. L., Washenfelder, R. A., Young, C. J., Gilman, J. B., De Gouw, J. A., Flynn, J. H., Grossberg, N., Lefer, B. L., Liu, J., Weber, R. J., and Osthoff, H. D.: Heterogeneous formation of nitryl chloride and its role as a nocturnal NO_x reservoir species during CalNex-LA 2010, J. Geophys. Res.-Atmos., 118, 10638–10652, https://doi.org/10.1002/jgrd.50783, 2013.

Molina, M. J. and Rowland, F. S.: Stratospheric sink for chlorofluoromethanes: Chlorine atom-catalysed destruction of ozone, Nature, 249, 810–812, https://doi.org/10.1038/249810a0, 1974.

Murphy, B. N., Donahue, N. M., Fountoukis, C., Dall'Osto, M., O'Dowd, C., Kiendler-Scharr, A., and Pandis, S. N.: Functionalization and fragmentation during ambient organic aerosol aging: application of the 2-D volatility basis set to field studies, Atmos. Chem. Phys., 12, 10797–10816, https://doi.org/10.5194/acp-12-10797-2012, 2012.

Nah, T., McVay, R. C., Pierce, J. R., Seinfeld, J. H., and Ng, N. L.: Constraining uncertainties in particle-wall deposition correction during SOA formation in chamber experiments, Atmos. Chem. Phys., 17, 2297–2310, https://doi.org/10.5194/acp-17-2297-2017, 2017.

Ng, N. L., Kroll, J. H., Chan, A. W. H., Chhabra, P. S., Flagan, R. C., and Seinfeld, J. H.: Secondary organic aerosol formation from m-xylene, toluene, and benzene, Atmos. Chem. Phys., 7, 3909–3922, https://doi.org/10.5194/acp-7-3909-2007, 2007.

Ng, N. L., Canagaratna, M. R., Zhang, Q., Jimenez, J. L., Tian, J., Ulbrich, I. M., Kroll, J. H., Docherty, K. S., Chhabra, P. S., Bahreini, R., Murphy, S. M., Seinfeld, J. H., Hildebrandt, L., Donahue, N. M., DeCarlo, P. F., Lanz, V. A., Prévôt, A. S. H., Dinar, E., Rudich, Y., and Worsnop, D. R.: Organic aerosol components observed in Northern Hemispheric datasets from Aerosol Mass Spectrometry, Atmos. Chem. Phys., 10, 4625–4641, https://doi.org/10.5194/acp-10-4625-2010, 2010.

Ng, N. L., Herndon, S. C., Trimborn, A., Canagaratna, M. R., Croteau, P. L., Onasch, T. B., Sueper, D., Worsnop, D. R., Zhang, Q., Sun, Y. L., and Jayne, J. T.: An Aerosol Chemical Speciation Monitor (ACSM) for routine monitoring of the composition and mass concentrations of ambient aerosol, Aerosol Sci. Technol., 45, 780–794, https://doi.org/10.1080/02786826.2011.560211, 2011a.

Ng, N. L., Canagaratna, M. R., Jimenez, J. L., Chhabra, P. S., Seinfeld, J. H., and Worsnop, D. R.: Changes in organic aerosol composition with aging inferred from aerosol mass spectra, Atmos. Chem. Phys., 11, 6465–6474, https://doi.org/10.5194/acp-11-6465-2011, 2011b.

Nguyen, T. B., Coggon, M. M., Bates, K. H., Zhang, X., Schwantes, R. H., Schilling, K. A., Loza, C. L., Flagan, R. C., Wennberg, P. O., and Seinfeld, J. H.: Organic aerosol formation from the reactive uptake of isoprene epoxydiols (IEPOX) onto non-acidified inorganic seeds, Atmos. Chem. Phys., 14, 3497–3510, https://doi.org/10.5194/acp-14-3497-2014, 2014.

Nordmeyer, T., Wang, W., Ragains, M. L., Finlayson-Pitts, B. J., Spicer, C. W., and Plastridge, R. A.: Unique products of the reaction of isoprene with atomic chlorine: Potential markers of chlorine atom chemistry, Geophys. Res. Lett., 24, 1615–1618, https://doi.org/10.1029/97GL01547, 1997.

O'Dowd, C. D. and de Leeuw, G.: Marine aerosol production: A review of the current knowledge, Phil. Trans. R. Soc. A, 365, 1753–1774, https://doi.org/10.1098/rsta.2007.2043, 2007.

Odum, J. R., Hoffmann, T., Bowman, F., Collins, D., Flagan Richard, C., and Seinfeld John, H.: Gas particle partitioning and secondary organic aerosol yields, Environ. Sci. Technol., 30, 2580–2585, https://doi.org/10.1021/es950943+, 1996.

Ofner, J., Balzer, N., Buxmann, J., Grothe, H., Schmitt-Kopplin, Ph., Platt, U., and Zetzsch, C.: Halogenation processes of secondary organic aerosol and implications on halogen release mechanisms, Atmos. Chem. Phys., 12, 5787–5806, https://doi.org/10.5194/acp-12-5787-2012, 2012.

Ofner, J., Kamilli, K. A., Held, A., Lendl, B., and Zetzsch, C.: Halogen-induced organic aerosol (XOA): A study on ultra-fine particle formation and time-resolved chemical characterization, Faraday Discuss., 165, 115–135, https://doi.org/10.1039/c3fd00093a, 2013.

Orlando, J. J., Tyndall, G. S., Apel, E. C., Riemer, D. D., and Paulson, S. E.: Rate coefficients and mechanisms of the reaction of Cl-atoms with a series of unsaturated hydrocarbons under atmospheric conditions, Int. J. Chem. Kinet., 35, 334–353, https://doi.org/10.1002/kin.10135, 2003.

Osthoff, H. D., Roberts, J. M., Ravishankara, A. R., Williams, E. J., Lerner, B. M., Sommariva, R., Bates, T. S., Coffman, D., Quinn, P. K., Dibb, J. E., Stark, H., Burkholder, J. B., Talukdar, R. K., Meagher, J., Fehsenfeld, F. C., and Brown, S. S.: High levels of nitryl chloride in the polluted subtropical marine boundary layer, Nat. Geosci., 1, 324–328, https://doi.org/10.1038/ngeo177, 2008.

Pankow, J. F.: An absorption model of gas/particle partitioning of organic compounds in the atmosphere, Atmos. Environ., 28, 185–188, https://doi.org/10.1016/1352-2310(94)90093-0, 1994.

Parrish, D. D., Allen, D. T., Bates, T. S., Estes, M., Fehsenfeld, F. C., Feingold, G., Ferrare, R., Hardesty, R. M., Meagher, J. F., Nielsen-Gammon, J. W., Pierce, R. B., Ryerson, T. B., Seinfeld, J. H., and Williams, E. J.: Overview of the second texas air quality study (TexAQS II) and the Gulf of Mexico atmospheric composition and climate study (GoMACCS), J. Geophys. Res.-Atmos., 114, 1–28, https://doi.org/10.1029/2009JD011842, 2009.

Pathak, R. K., Presto, A. A., Lane, T. E., Stanier, C. O., Donahue, N. M., and Pandis, S. N.: Ozonolysis of α-pinene: parameterization of secondary organic aerosol mass fraction, Atmos. Chem. Phys., 7, 3811–3821, https://doi.org/10.5194/acp-7-3811-2007, 2007.

Paulot, F., Crounse, J. D., Kjaergaard, H. G., Kroll, J. H., Seinfeld, J. H., and Wennberg, P. O.: Isoprene photooxidation: new insights into the production of acids and organic nitrates, Atmos. Chem. Phys., 9, 1479–1501, https://doi.org/10.5194/acp-9-1479-2009, 2009.

Pierce, J. R., Engelhart, G. J., Hildebrandt, L., Weitkamp, E. A., Pathak, R. K., Donahue, N. M., Robinson, A. L., Adams, P. J., and Pandis, S. N.: Constraining particle evolution from wall losses, coagulation, and condensation-evaporation in smog-chamber experiments: Optimal estimation based on size distribution measurements, Aerosol Sci. Technol., 42, 1001–1015, https://doi.org/10.1080/02786820802389251, 2008.

Platt, U. and Hönninger, G.: The role of halogen species in the troposphere, Chemosphere, 52, 325–338, https://doi.org/10.1016/S0045-6535(03)00216-9, 2003.

Pöhler, D., Vogel, L., Friess, U., and Platt, U.: Observation of halogen species in the Amundsen Gulf, Arctic, by active long-path differential optical absorption spectroscopy, P. Natl. Acad. Sci., 107, 6582–6587, https://doi.org/10.1073/pnas.0912231107, 2010.

Pope, C. A., Dockery, D. W., Chow, J. C., Watson, J. G., Mauderly, J. L., Costa, D. L., Wyzga, R. E., Vedal, S., Hidy, G. M., Altshuler, S. L., Marrack, D., Heuss, J. M., Wolff, G. T., and Arden Pope III, C.: Health effects of fine particulate air pollution: Lines that connect, J. Air Waste Manage. Assoc., 56, 1368–1380, https://doi.org/10.1080/10473289.2006.10464485, 2006.

Ragains, M. L. and Finlayson-Pitts, B. J.: Kinetics and mechanism of the reaction of Cl atoms with 2-methyl-1,3-butadiene (isoprene) at 298 K, J. Phys. Chem. A, 101, 1509–1517, https://doi.org/10.1021/jp962786m, 1997.

Read, K. A., Mahajan, A. S., Carpenter, L. J., Evans, M. J., Faria, B. V. E., Heard, D. E., Hopkins, J. R., Lee, J. D., Moller, S. J., Lewis, A. C., Mendes, L., McQuaid, J. B., Oetjen, H., Saiz-Lopez, A., Pilling, M. J., and Plane, J. M. C.: Extensive halogen-mediated ozone destruction over the tropical Atlantic Ocean, Nature, 453, 1232–1235, https://doi.org/10.1038/nature07035, 2008.

Riedel, T. P., Bertram, T. H., Crisp, T. A., Williams, E. J., Lerner, B. M., Vlasenko, A., Li, S. M., Gilman, J., De Gouw, J., Bon, D. M., Wagner, N. L., Brown, S. S., and Thornton, J. A.: Nitryl chloride and molecular chlorine in the coastal marine boundary layer, Environ. Sci. Technol., 46, 10463–10470, https://doi.org/10.1021/es204632r, 2012.

Riedel, T. P., Wagner, N. L., Dubé, W. P., Middlebrook, A. M., Young, C. J., Öztürk, F., Bahreini, R., Vandenboer, T. C., Wolfe, D. E., Williams, E. J., Roberts, J. M., Brown, S. S., and Thornton, J. A.: Chlorine activation within urban or power plant plumes: Vertically resolved $ClNO_2$ and Cl_2 measurements from a tall tower in a polluted continental setting, J. Geophys. Res.-Atmos., 118, 8702–8715, https://doi.org/10.1002/jgrd.50637, 2013.

Riedel, T. P., Wolfe, G. M., Danas, K. T., Gilman, J. B., Kuster, W. C., Bon, D. M., Vlasenko, A., Li, S.-M., Williams, E. J., Lerner, B. M., Veres, P. R., Roberts, J. M., Holloway, J. S., Lefer, B., Brown, S. S., and Thornton, J. A.: An MCM modeling study of nitryl chloride ($ClNO_2$) impacts on oxidation, ozone production and nitrogen oxide partitioning in polluted continental outflow, Atmos. Chem. Phys., 14, 3789–3800, https://doi.org/10.5194/acp-14-3789-2014, 2014.

Riedel, T. P., Lin, Y. H., Budisulistiorini, S. H., Gaston, C. J., Thornton, J. A., Zhang, Z., Vizuete, W., Gold, A., and Surratt, J. D.: Heterogeneous reactions of isoprene-derived epoxides: Reaction probabilities and molar secondary organic aerosol yield estimates, Environ. Sci. Technol. Lett., 2, 38–42, https://doi.org/10.1021/ez500406f, 2015.

Riedel, T. P., Lin, Y.-H., Zhang, Z., Chu, K., Thornton, J. A., Vizuete, W., Gold, A., and Surratt, J. D.: Constraining condensed-phase formation kinetics of secondary organic aerosol components from isoprene epoxydiols, Atmos. Chem. Phys., 16, 1245–1254, https://doi.org/10.5194/acp-16-1245-2016, 2016.

Riemer, D. D., Apel, E. C., Orlando, J. J., Tyndall, G. S., Brune, W. H., Williams, E. J., Lonneman, W. A., and Neece, J. D.: Unique isoprene oxidation products demonstrate chlorine atom chemistry occurs in the Houston, Texas urban area, J. Atmos. Chem., 61, 227–242, https://doi.org/10.1007/s10874-009-9134-5, 2008.

Riva, M., Healy, R. M., Flaud, P. M., Perraudin, E., Wenger, J. C., and Villenave, E.: Gas- and particle-phase products from the chlorine-initiated oxidation of polycyclic aromatic hydrocarbons, J. Phys. Chem. A, 119, 11170–11181, https://doi.org/10.1021/acs.jpca.5b04610, 2015.

Riva, M., Budisulistiorini, S. H., Chen, Y., Zhang, Z., D'Ambro, E. L., Zhang, X., Gold, A., Turpin, B. J., Thornton, J. A., Canagaratna, M. R., and Surratt, J. D.: Chemical characterization of secondary organic aerosol from oxidation of isoprene hydroxyhydroperoxides, Environ. Sci. Technol., 50, 9889–9899, https://doi.org/10.1021/acs.est.6b02511, 2016.

Saiz-Lopez, A. and von Glasow, R.: Reactive halogen chemistry in the troposphere, Chem. Soc. Rev., 41, 6448, https://doi.org/10.1039/c2cs35208g, 2012.

Sarwar, G., Simon, H., Bhave, P., and Yarwood, G.: Examining the impact of heterogeneous nitryl chloride production on air quality across the United States, Atmos. Chem. Phys., 12, 6455–6473, https://doi.org/10.5194/acp-12-6455-2012, 2012.

Schwantes, R. H., Teng, A. P., Nguyen, T. B., Coggon, M. M., Crounse, J. D., St. Clair, J. M., Zhang, X., Schilling, K. A., Seinfeld, J. H., and Wennberg, P. O.: Isoprene NO_3 oxidation products from the $RO_2 + HO_2$ pathway, J. Phys. Chem. A, 119, 10158–10171, https://doi.org/10.1021/acs.jpca.5b06355, 2015.

Simpson, W. R., Brown, S. S., Saiz-Lopez, A., Thornton, J. A., and Von Glasow, R.: Tropospheric halogen chemistry: Sources, cycling, and impacts, Chem. Rev., 115, 4035–4062, https://doi.org/10.1021/cr5006638, 2015.

Stutz, J.: Atmospheric reactive chlorine and bromine at the Great Salt Lake, Utah, Geophys. Res. Lett., 29, 18–21, https://doi.org/10.1029/2002GL014812, 2002.

Surratt, J. D., Murphy, S. M., Kroll, J. H., Ng, N. L., Hildebrandt, L., Sorooshian, A., Szmigielski, R., Vermeylen, R., Maenhaut, W., Claeys, M., Flagan, R. C., and Seinfeld, J. H.: Chemical composition of secondary organic aerosol formed from the photooxidation of isoprene, J. Phys. Chem. A, 110, 9665–9690, https://doi.org/10.1021/jp061734m, 2006.

Surratt, J. D., Chan, A. W., Eddingsaas, N. C., Chan, M., Loza, C. L., Kwan, A. J., Hersey, S. P., Flagan, R. C., Wennberg, P. O., and Seinfeld, J. H.: Reactive intermediates revealed in secondary organic aerosol formation from isoprene, P. Natl. Acad. Sci., 107, 6640–6645, https://doi.org/10.1073/pnas.0911114107, 2010.

Tanaka, P. L. and Allen, D. T.: Incorporation of Chlorine Reactions into the Carbon Bond-IV Mechanism (supplement), available at: https://www.tceq.texas.gov/assets/public/implementation/air/am/contracts/reports/oth/IncorporationOfChlorineReactionsIntoCB4-2.pdf (last access: 4 October 2017), 2001.

Tanaka, P. L., Riemer, D. D., Chang, S., Yarwood, G., McDonald-Buller, E. C., Apel, E. C., Orlando, J. J., Silva, P. J., Jimenez, J. L., Canagaratna, M. R., Neece, J. D., Mullins, C. B., and Allen, D. T.: Direct evidence for chlorine-enhanced urban ozone formation in Houston, Texas, Atmos. Environ., 37, 1393–1400, https://doi.org/10.1016/S1352-2310(02)01007-5, 2003.

Thornton, J. A., Kercher, J. P., Riedel, T. P., Wagner, N. L., Cozic, J., Holloway, J. S., Dubé, W. P., Wolfe, G. M., Quinn, P. K., Middlebrook, A. M., Alexander, B., and Brown, S. S.: A large atomic chlorine source inferred from mid-continental reactive nitrogen chemistry, Nature, 464, 271–4, https://doi.org/10.1038/nature08905, 2010.

Ulbrich, I. M., Canagaratna, M. R., Zhang, Q., Worsnop, D. R., and Jimenez, J. L.: Interpretation of organic components from Positive Matrix Factorization of aerosol mass spectrometric data, Atmos. Chem. Phys., 9, 2891–2918, https://doi.org/10.5194/acp-9-2891-2009, 2009.

Verheggen, B. and Mozurkewich, M.: An inverse modeling procedure to determine particle growth and nucleation rates from measured aerosol size distributions, Atmos. Chem. Phys., 6, 2927–2942, https://doi.org/10.5194/acp-6-2927-2006, 2006.

Wang, D. S. and Hildebrandt Ruiz, L.: Secondary organic aerosol from chlorine-initiated oxidation of isoprene, https://doi.org/10.18738/T8/DVALR9, Texas Data Repository Dataverse, V2, 2017, last access: 10 November 2017.

Wang, L., Arey, J., and Atkinson, R.: Reactions of chlorine atoms with a series of aromatic hydrocarbons, Environ. Sci. Technol., 39, 5302–5310, https://doi.org/10.1021/es0479437, 2005.

Wingenter, O. W., Blake, D. R., Blake, N. J., Sive, B. C., Rowland, F. S., Atlas, E., and Flocke, F.: Tropospheric hydroxyl and atomic chlorine concentrations, and mixing timescales determined from hydrocarbon and halocarbon measurements made over the Southern Ocean, J. Geophys. Res., 104, 21819, https://doi.org/10.1029/1999JD900203, 1999.

Wingenter, O. W., Sive, B. C., Blake, N. J., Blake, D. R., and Rowland, F. S.: Atomic chlorine concentrations derived from ethane and hydroxyl measurements over the equatorial Pacific Ocean: Implication for dimethyl sulfide and bromine monoxide, J. Geophys. Res.-Atmos., 110, 1–10, https://doi.org/10.1029/2005JD005875, 2005.

Xu, L., Kollman, M. S., Song, C., Shilling, J. E., and Ng, N. L.: Effects of NO_x on the volatility of secondary organic aerosol from isoprene photooxidation, Environ. Sci. Technol., 48, 2253–2262, https://doi.org/10.1021/es404842g, 2014.

Yarwood, G., Jung, J., Whitten, G. Z., Heo, G., Mellberg, J., and Estes, M.: Updates to the Carbon Bond mechanism for version 6 (CB6), presented at the 9th Annual CMAS Conference, Chapel Hill, NC, 11–13 October, vol. 6, 1–4, 2010.

Yatavelli, R. L. N., Lopez-Hilfiker, F., Wargo, J. D., Kimmel, J. R., Cubison, M. J., Bertram, T. H., Jimenez, J. L., Gonin, M., Worsnop, D. R., and Thornton, J. A.: A Chemical Ionization High-Resolution Time-of-Flight Mass Spectrometer coupled to a Micro Orifice Volatilization Impactor (MOVI-HRToF-CIMS) for analysis of gas and particle-phase organic species, Aerosol Sci. Technol., 46, 1313–1327, https://doi.org/10.1080/02786826.2012.712236, 2012.

Young, C. J., Washenfelder, R. A., Edwards, P. M., Parrish, D. D., Gilman, J. B., Kuster, W. C., Mielke, L. H., Osthoff, H. D., Tsai, C., Pikelnaya, O., Stutz, J., Veres, P. R., Roberts, J. M., Griffith, S., Dusanter, S., Stevens, P. S., Flynn, J., Grossberg, N., Lefer, B., Holloway, J. S., Peischl, J., Ryerson, T. B., Atlas, E. L., Blake, D. R., and Brown, S. S.: Chlorine as a primary radical: evaluation of methods to understand its role in initiation of oxidative cycles, Atmos. Chem. Phys., 14, 3427–3440, https://doi.org/10.5194/acp-14-3427-2014, 2014.

Zhang, X., Schwantes, R. H., McVay, R. C., Lignell, H., Coggon, M. M., Flagan, R. C., and Seinfeld, J. H.: Vapor wall deposition in Teflon chambers, Atmos. Chem. Phys., 15, 4197–4214, https://doi.org/10.5194/acp-15-4197-2015, 2015.

Zhao, B., Wang, S., Donahue, N. M., Chuang, W., Hildebrandt Ruiz, L., Ng, N. L., Wang, Y., and Hao, J.: Evaluation of one-dimensional and two-dimensional volatility basis sets in simulating the aging of secondary organic aerosol with smog-chamber experiments, Environ. Sci. Technol., 49, 2245–2254, https://doi.org/10.1021/es5048914, 2015.